Electronic Supplementary Information (ESI)

Ruthenium Bipyridyl Tethered Porous Organosilica: A Versatile, Durable, and Reusable Heterogeneous Photocatalyst

Avijit Jana,[a] John Mondal,[a] Parijat Borah,[a] Sujan Mondal,[b] Asim Bhaumik,*[,b] Yanli Zhao*[,a,c]

[a] Division of Chemistry and Biological Chemistry
School of Physical and Mathematical Sciences
Nanyang Technological University
121 Nanyang Link, Singapore 637371
E-mail: zhaoyanli@ntu.edu.sg

[b] Department of Materials Science
Indian Association for the Cultivation of Science
Jadavpur 700 032, India
E-mail: msab@iacs.res.in

[c] School of Materials Science and Engineering
Nanyang Technological University
50 Nanyang Avenue, Singapore 639798

General information. All reagents were purchased from Sigma-Aldrich and used without further purification. ^{1}H NMR spectra were recorded on a Bruker-AC 300 MHz spectrometer. Chemical shifts are reported in ppm from tetramethylsilane with the solvent resonance as the internal standard (deuterochloroform: 7.26 ppm). Data are reported as follows: chemical shifts, multiplicity (s = singlet, d = doublet, t = triplet, m = multiplet), and coupling constant (Hz). ^{13}C NMR (75 MHz) spectra were recorded on a Bruker-AC 300 MHz spectrometer with complete proton decoupling. Chemical shifts are reported in ppm from tetramethylsilane with the solvent resonance as the internal standard (deuterochloroform: 77.0 ppm). Fluorescence emission spectra were recorded on a Shimadzu RF-5301 PC spectrofluorophotometer. FT-IR spectra were recorded on a Perkin Elmer RXI spectrometer. Quadrupole ion trap mass spectrometer equipped with Thermo Accela LC and Agilent 6890 GC system equipped with a flame ionization detector were used for analysis of catalytic reactions. Ru loading in the sample was estimated by using a Perkin-Elmer Optima 2100 DV Inductive Coupled Plasma Mass Spectroscopy (ICP-MS). Transmission electron microscopy images were measured on a JEM-1400 (JEOL) operated at 100-120 kV and high resolution transmittance electron microscopic (HR-TEM) images were recorded in a JEOL JEM 2010 transmission electron microscope. The TEM samples were

prepared by dispersing materials in methanol, and the suspension was dropped on the surface of a copper grid. X-ray photoelectron spectroscopy (XPS) analysis was carried out by a SPECS I3500 plus spectrometer using Mg X-ray source. Chromatographic purification was performed with 60-120 mesh silica gel (Merck). For monitoring reactions, precoated silica gel 60 F254 TLC sheets (Merck) were used.

Synthesis of 2,2'-bipyridine-4,4'-dicarboxylic acid (2).[1,2] In a 100 mL round-bottomed flask, 4,4'-dimethyl-2,2'- bipyridine (5.0 g, 27.1 mmol) was dissolved in conc. sulfuric acid (30 mL), and the solution was cooled at 0 °C. To the solution was added CrO_3 (16.2 g, 160 mmol) in portion under vigorous stirring, and the resulting dark blue mixture was stirred at 80 °C for 8 h and then at room temperature overnight. The mixture was poured into crashed ice (ca. 200 mL), and the resulting white precipitate was collected by filtration. This solid was dissolved in NaOH aqueous solution (1 g / 20 mL), and the insoluble materials were removed by filtration. The filtrate was neutralized with 5M HCl, and the resulting white precipitates were washed with water, methanol, and Et_2O, and finally dried (5.49 g, 83 %).

Synthesis of dimethyl[2,2'-bipyridine]-4,4'-dicarboxylate (3).[1,2] To a suspension of 4,4′-dicarboxy-2,2′-bipyridine (5.0 g, 20.5 mmol) in absolute methanol (400 mL) was added concentrated sulfuric acid (5 mL). The mixture was refluxed for 80 h to obtain a clear solution and then cooled to room temperature. Water (400 mL) was added and the excess methanol was removed under vacuum. The pH was adjusted to neutral with NaOH solution, and the resulting precipitate was filtered and washed with water (pH = 7). The solid was dried to obtain **3** (5.5 g, 90%). ^{1}H NMR ($CDCl_3$, 300 MHz) δ = 8.94 (s, 2H), 8.85-8.83 (d, J = 5.7 Hz, 2H), 7.88-7.87 (d, J = 4.8 Hz, 2H), 3.98 (s, 6H); ^{13}C NMR ($CDCl_3$, 75 Hz) δ = 165.6, 156.5, 150.1, 138.6, 123.2, 120.5, 52.7.

Synthesis of [2,2'-bipyridine]-4,4'-diyldimethanol (4).[1,2] Sodium borohydride (1.0 g) was added in one portion to a suspension of the diester **3** (5.5 g, 20.2 mmol) in absolute methanol (200 mL). The mixture was refluxed for 3 h and then cooled to room temperature. An ammonium chloride saturated water solution (200 mL) was added to decompose the excess borohydride. The methanol was removed under vacuum and the precipitated solid was dissolved in a minimal amount of water. The resulting solution was extracted with ethyl acetate (5 × 200 mL) and dried over sodium sulfate, and the solvent was removed under vacuum. The desired solid **4** was obtained in 79% yield and was used without further purification. ^{1}H NMR (CD_3OD, 300 MHz) δ

= 8.57-8.55 (d, J = 5.1 Hz, 2H), 8.24 (s, 2H), 7.42-7.39 (m, 2H), 4.72 (s, 4H); ^{13}C NMR (CD_3OD, 75 Hz) δ = 155.8, 152.9, 148.7, 121.3, 118.8, 62.2.

Synthesis of the ligand [2,2'-bipyridine]-4,4'-diylbis(methylene) bis((3-(triethoxysilyl) propyl)carbamate) (5): Compound **4** (0.648 g, 3.0 mmol) was dissolved in dry DMF (5 mL) followed by the addition of triethoxy(3-isocyanatopropyl)silane (1.482 g, 6.0 mmol). The reaction mixture was heated at 90 ˚C under constant stirring overnight. After completion of the reaction (monitored by LCMS), the solvent was removed under vacuum using rotary evaporator to yield the ligand **5** as viscous oil, which was directly used for the complexation reaction with $RuCl_3$ without further purification.

Synthesis of tris[2,2'-bipyridine]-4,4'-diylbis(methylene)bis((3-(triethoxysilyl)propyl) carbamate)]ruthenium(ii) chloride (6):[1,2] The complex **6** was synthesized following the standard protocol. The ligand **5** (2.13 g, 3 mmol) was dissolved in dry EtOH (50 mL) and dry $RuCl_3$ (0.207 g, 1 mmol) was added followed by the addition of sodium hypophohphite (NaH_2PO_2, 0.132 g, 1.5 mmol). The reaction mixture was refluxed for 3 h followed by evaporation of solvent to obtain the desired complex **6** as bright orange viscous liquid, which was directly used for the preparation of Ru-POS without further purification.

Synthesis of Ru-POS: Cetyltrimethylammonium bromide (CTAB) was used as a structure-directing agent for the synthesis of Ru-POS material. In a typical synthesis procedure, CTAB (15.0 mmol, 0.546 g) was dissolved in water (10 mL) under vigorous stirring conditions at room temperature to attain a clear solution. Then, dark red colored viscous organosilane precursor (1.0 mmol, 2.304 g) was added drop wise into the previously prepared surfactant solution and the reaction mixture was allowed to stir for about 2 h. After that, tetraethyl orthosilicate (TEOS, 9.0 mmol, 1.872 g) was added into the reaction mixture and it was stirred for about 2 h to obtain a dark red colored viscous gel. The pH of the reaction mixture was around 7.5. After 2 h stirring, the pH of the resulting gel was maintained to *ca.* 12 with the addition of 2 M NaOH solution. The resulting gel was stirred for another 12 h at room temperature and then it was treated hydrothermally at 353 K under static conditions for 72 h. The dark red colored solid was recovered under filtration, washed several times with water followed by ethanol, and dried under vacuum. The template CTAB was removed from the as-synthesized sample by extracting the solid sample two times with NH_4NO_3 in an ethanolic solution at room temperature. The finally obtained sample is designated as Ru-POS.

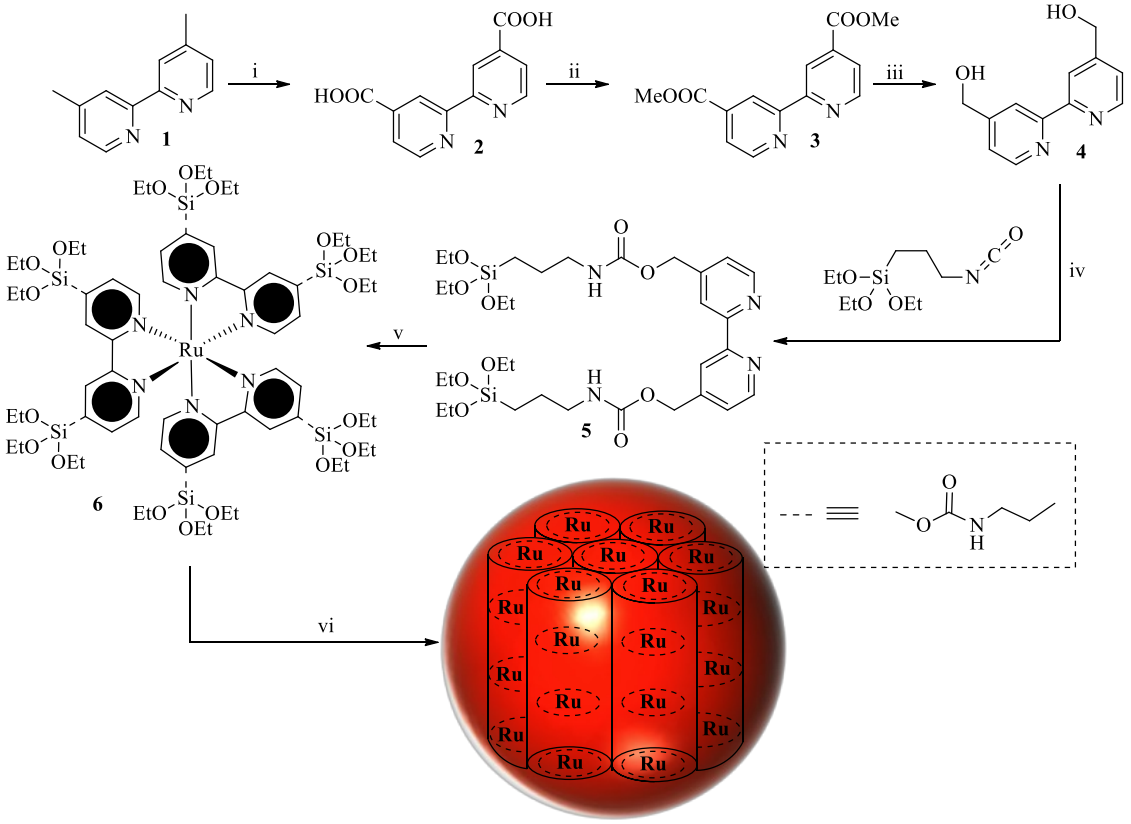

Scheme S1. Synthesis of Ru-POS. *Reagents and conditions:* (i) CrO_3, H_2SO_4, 80 ˚C, (ii) MeOH, H_2SO_4, reflux, (iii) $NaBH_4$, EtOH, reflux, (iv) DMF, 90 ˚C, (v) $RuCl_3$, NaH_2PO_2, EtOH reflux (vi) CTAB, TEOS.

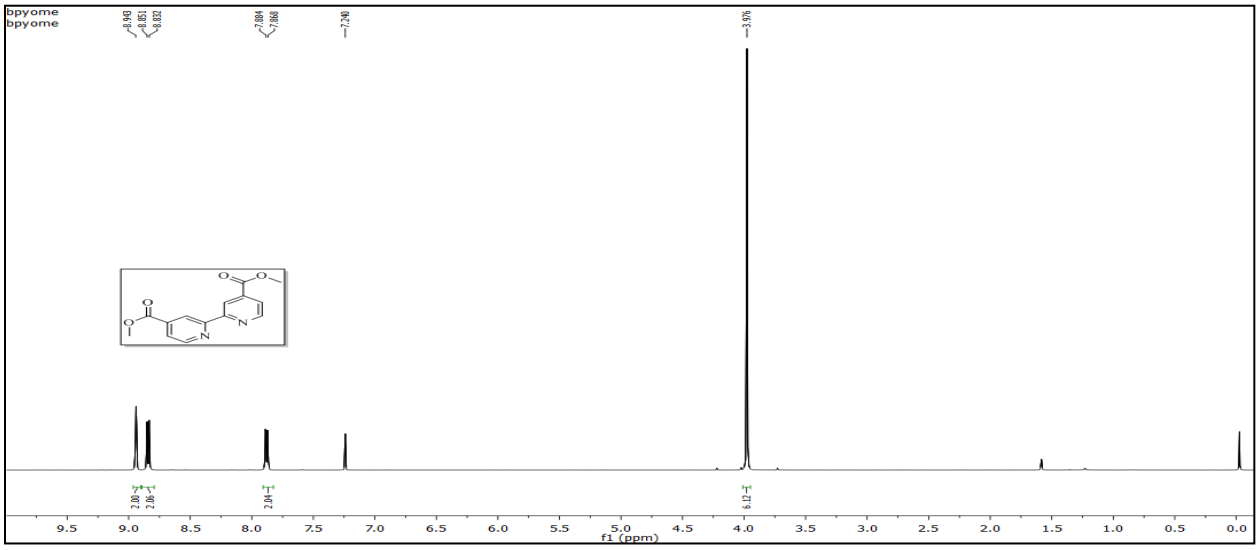

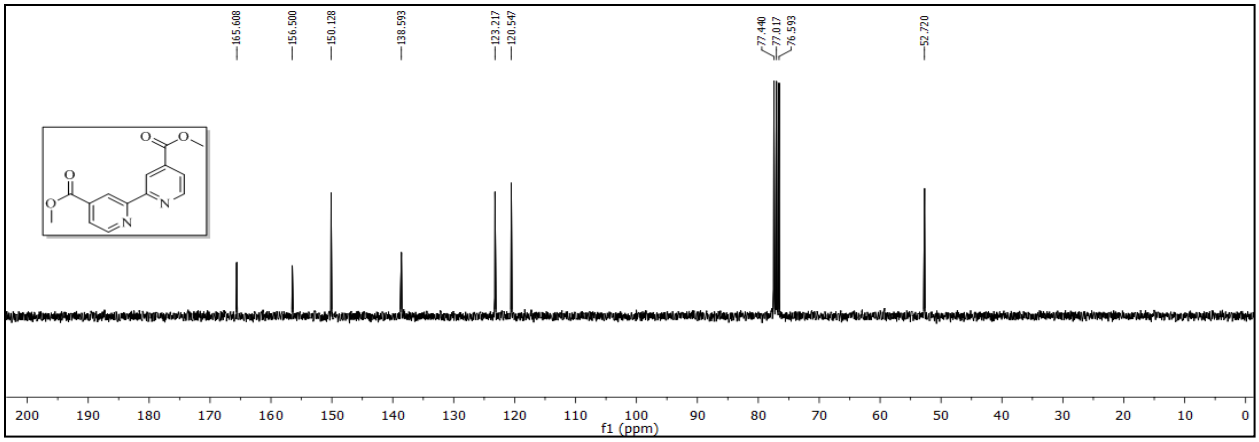
165.608
156.500
150.128
138.593
123.217
120.547
77.440
77.017
76.593
52.720
f1 (ppm)

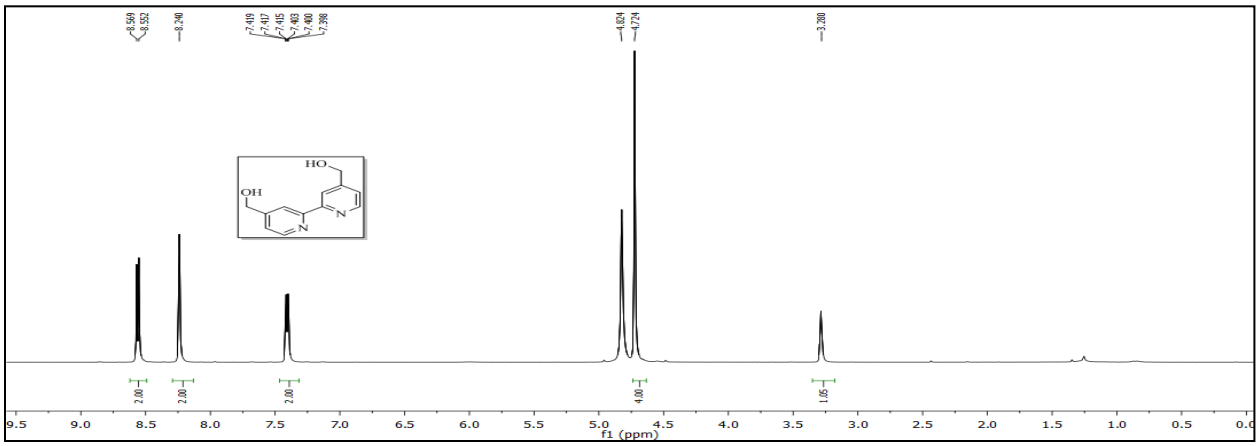
8.569
8.552
8.240
7.419
7.417
7.415
7.403
7.400
7.398
4.824
4.724
3.280
HO
OH
N
2.00
2.00
2.00
4.00
1.05
f1 (ppm)

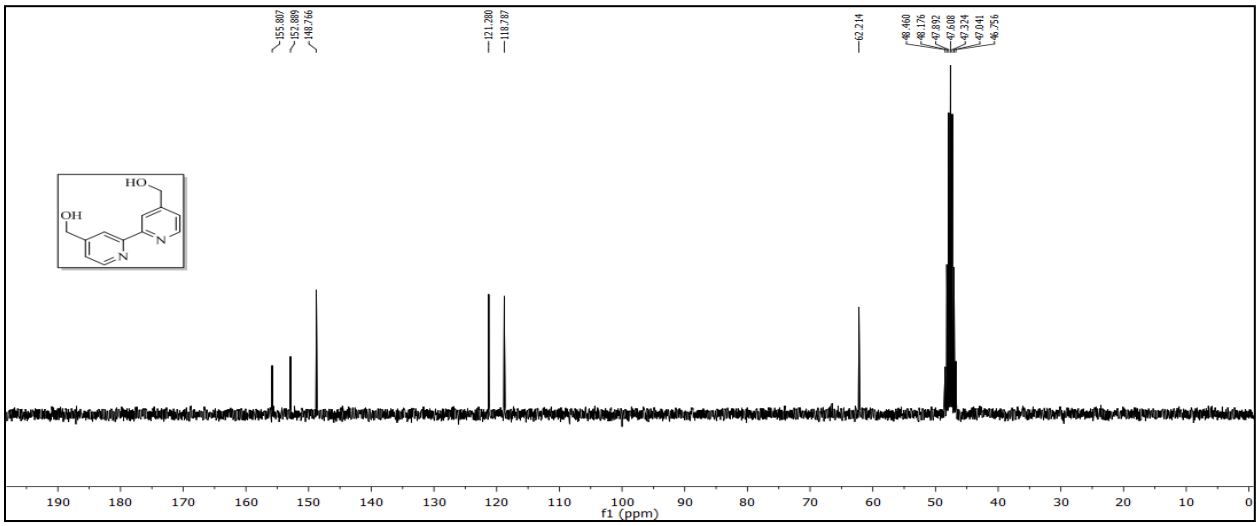
155.807
152.889
148.766
121.280
118.787
62.214
48.460
48.176
47.892
47.608
47.324
47.041
46.756
HO
OH
N
f1 (ppm)

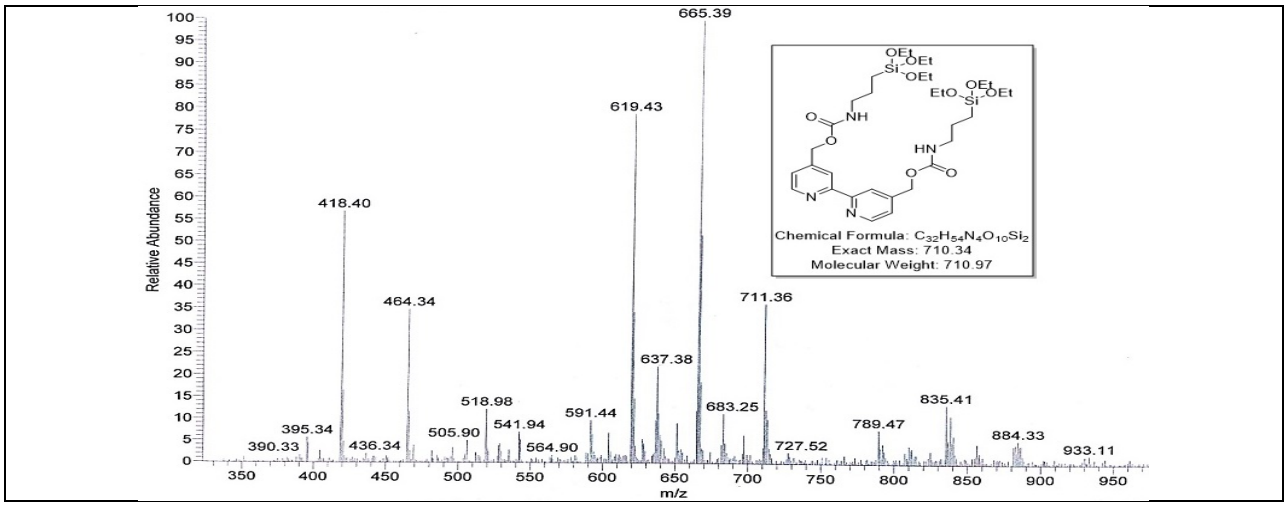

Characterization spectra for dimethyl [2,2'-bipyridine]-4,4'-dicarboxylate, [2,2'-bipyridine]-4,4'-diyldimethanol, and [2,2'-bipyridine]-4,4'-diylbis(methylene) bis((3-(triethoxysilyl) propyl)carbamate).

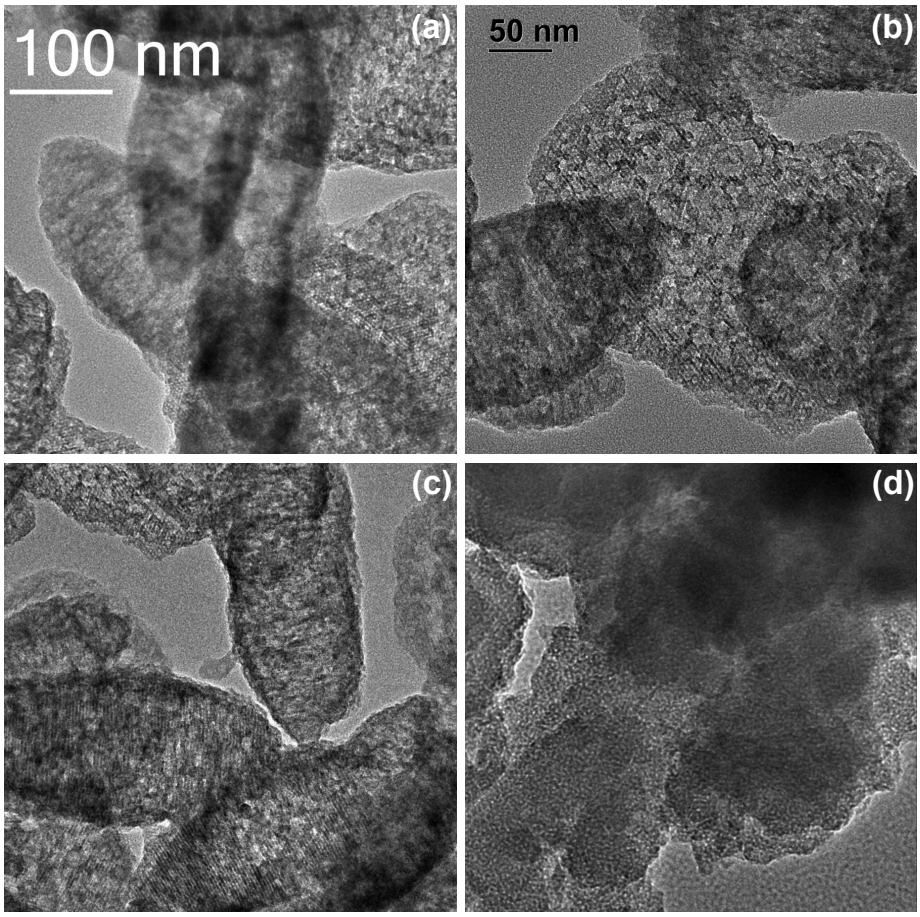

Figure S1. High resolution TEM images of Ru-POS: (a,b) electron beam parallel to the pore axis and (c) electron beam perpendicular to the pore axis. (d) High resolution TEM image for the used Ru-POS.

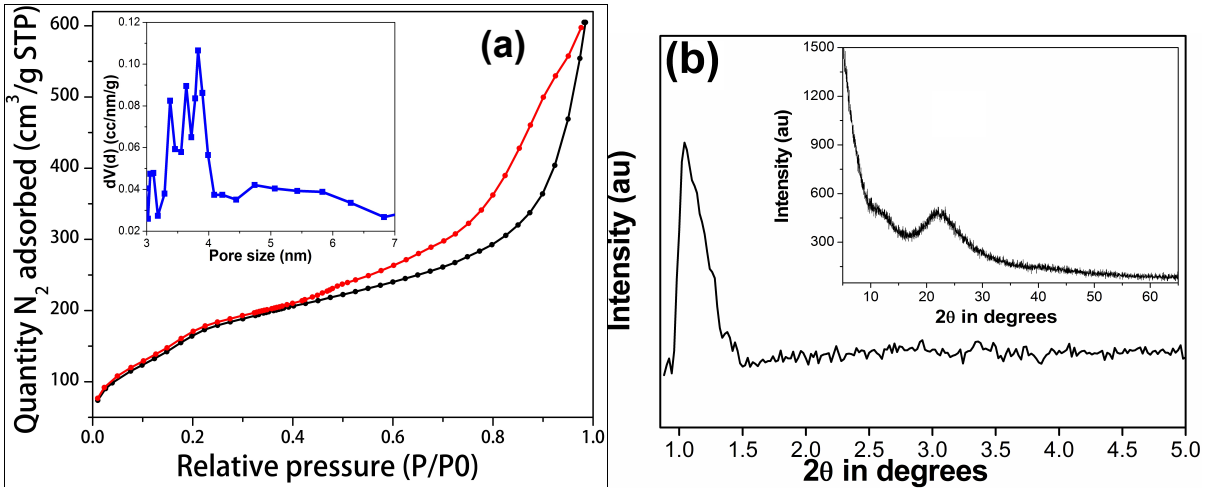

Figure S2. (a) N_2 adsorption/desorption isotherm of Ru-POS, and the inset shows the pore size distribution of the material. (b) Small angel powder XRD pattern of Ru-POS, and the inset shows wide angel powder XRD pattern of Ru-POS.

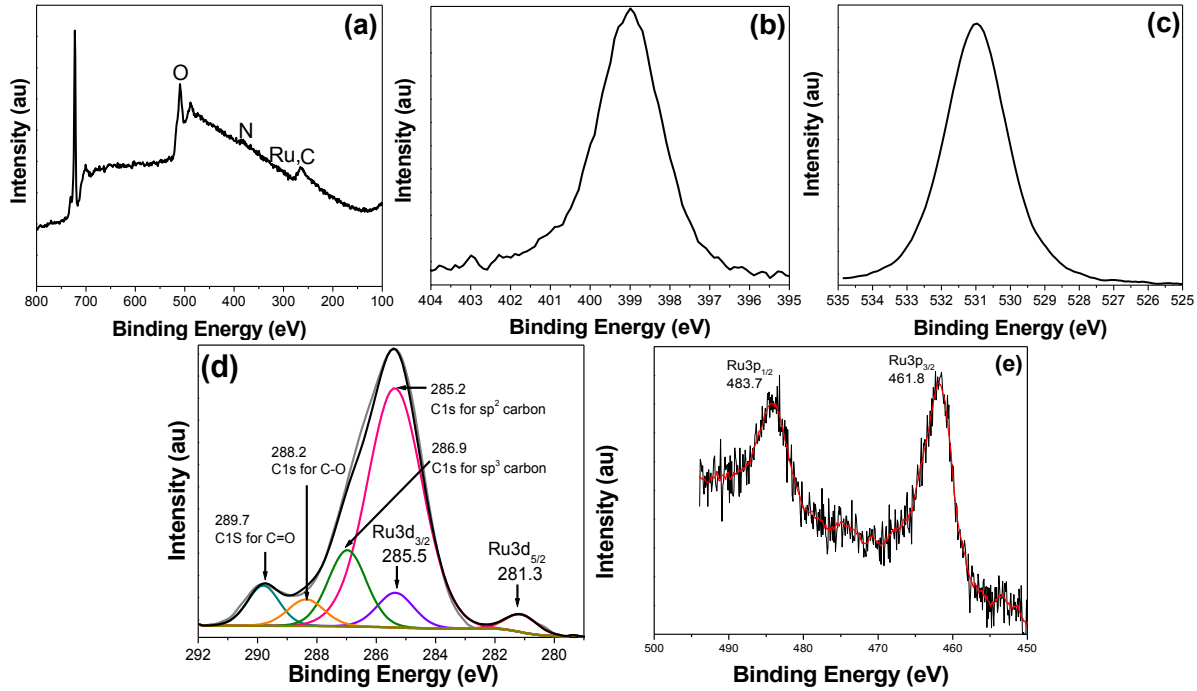

Figure S3. XPS spectra of Ru-POS: (a) Survey spectrum showing the presence of constituting elements, (b) XPS spectrum for nitrogen (N), (c) XPS spectrum for oxygen (O), (d) XPS spectra for Ru-POS after 10 catalytic cycles showing the peaks corresponding to $Ru3d_{5/2}$ and $3d_{3/2}$ (181.3 and 285.5 eV respectively) as well as C1s for different kinds of C atoms in Ru-POS, and (e) XPS spectrum for $Ru3p_{1/2}$ and $Ru3p_{3/2}$ in Ru-POS showing the peaks of binding energy at 483.7 eV and 461.8 eV respectively, further confirming the presence of ruthenium within Ru-POS.

XPS analysis: The XPS analysis of Ru-POS reveals the presence of constituting elements, *i.e.*, O, N, C and Ru (Figure S3). Since the C1s and Ru3d peaks in core level XPS spectrum overlap to each other, we deconvoluted the peaks to assign them for C and Ru. Peaks at 281.3 and 285.5 eV were assigned to $Ru3d_{5/2}$ and $Ru3d_{3/2}$ respectively, whereas other peaks such as 285.2, 286.9, 288.2 and 289.7 eV were assigned to C1s for different kinds of C atoms in Ru-POS (Figure S3d).

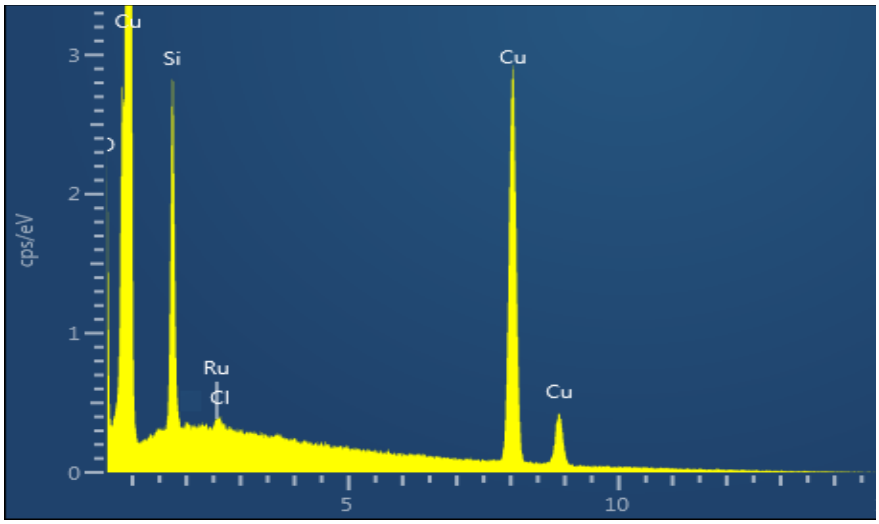

Figure S4. EDX pattern of Ru-POS showing the presence of Ru. The corresponding peaks for Cu appeared are because that the EDX analysis of Ru-POS was carried out on Cu grid.

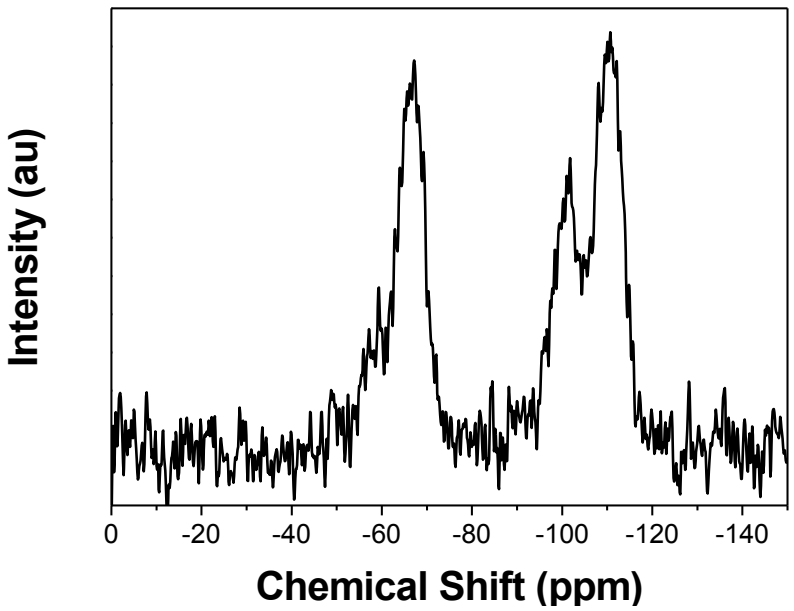

Figure S5. ^{29}Si MAS NMR spectrum of Ru-POS.

Solid state ^{29}Si NMR spectrum of Ru-POS: Solid state ^{29}Si NMR results provide useful information about the chemical environment of Si atoms and the presence of an organic functionality in the organic–inorganic hybrid frameworks of the mesoporous catalyst Ru-POS. Solid state ^{29}Si NMR spectrum (Figure S5) of Ru-POS exhibits two broad T^n and two Q^n signals with the chemical shifts at –59.0, -66.1, -101.7 and 110.8 ppm, which could be attributed to the T^2 [R–Si(OSi)$_2$(OH)], T^3 [(OSi)$_3$Si–R], Q^3 [Si(OSi)$_3$(OH)] and Q^4 [Si(OSi)$_4$] species, respectively.[3]

^{13}C CPMAS NMR spectrum of Ru-POS: The ^{13}C CP MAS NMR spectrum for the reused organocatalyst displays characteristic signals of aliphatic and aromatic carbons as shown in Figure S6.

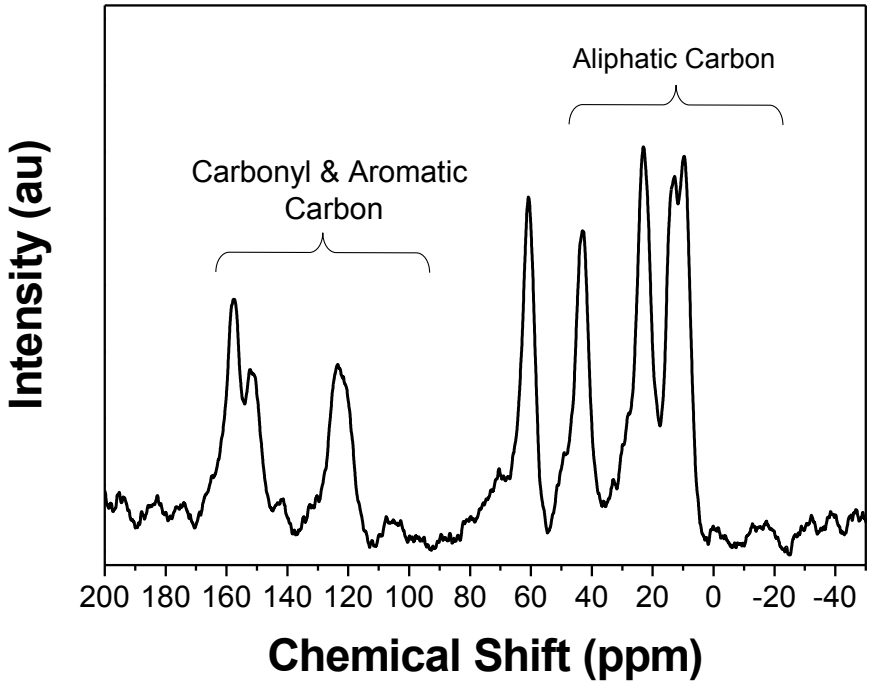

Figure S6. ^{13}C MAS NMR spectrum of reused Ru-POS.

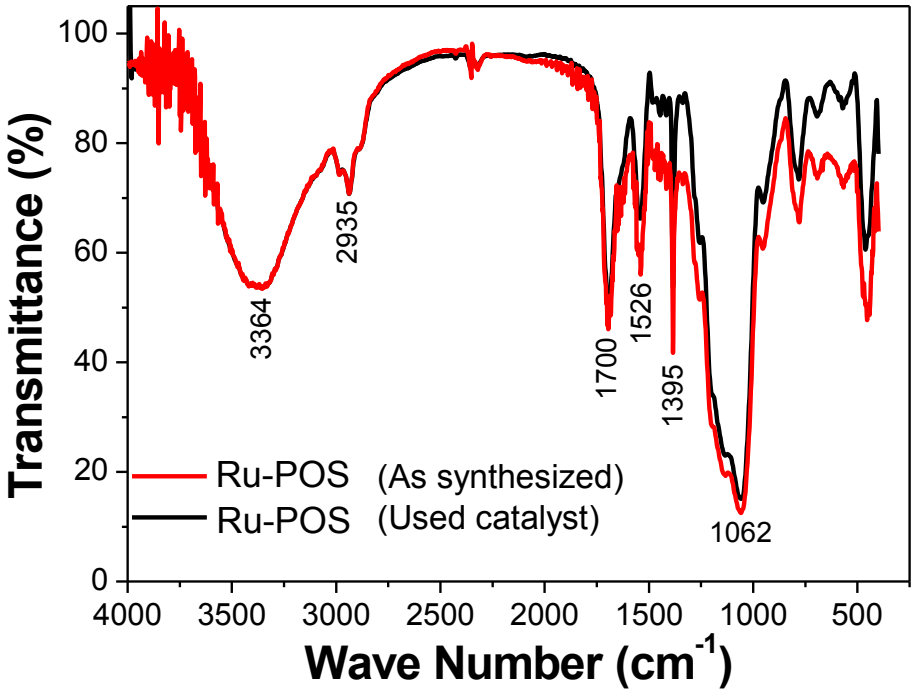

Figure S7. FT-IR spectra of Ru-POS before and after catalysis.

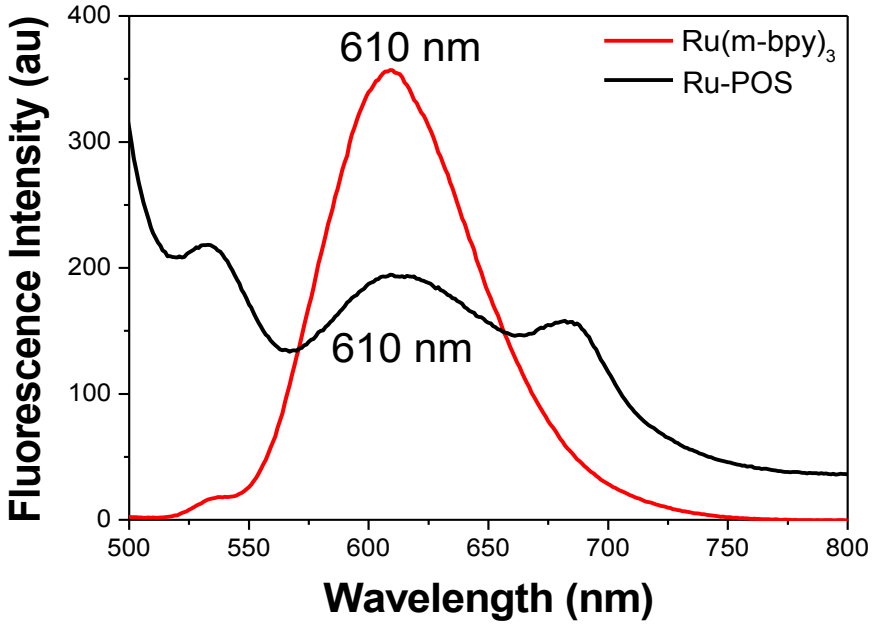

Figure S8. Emission spectra of [Ru(4,4'-dimethyl-2,2'-bipyridine)$_3$]Cl_2 (or Ru(m-bpy)$_3$) and Ru-POS.

Synthesis of 1,4-dihydropyridine derivatives: The corresponding 1,4-dihydropyridine derivatives were synthesized by following the literature procedure,[4] where triphenylphosphine was used as the catalyst (Scheme S2). After completion of the reaction, 1,4-dihydropyridine derivatives were isolated and purified by column chromatography.

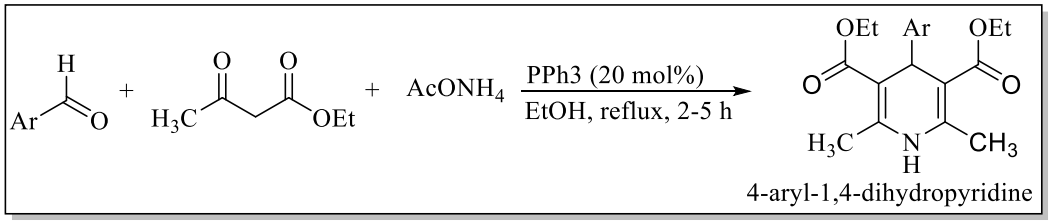

Scheme S2. Synthesis of 1,4-dihydropyridine derivatives.

Photo-catalytic oxidative aromatization of 1,4-dihydropyridine derivatives: As-synthesized 1,4-dihydropyridine derivatives (1 mmol) were subjected to photo-catalytic oxidative aromatization, where Ru-POS (20 mg) was added in acetonitrile suspension and irradiated using 25W compact fluorescent lamp for 2 h, resulting in the formation of the corresponding pyridine derivatives with excellent yields as acquired from GCMS analysis.

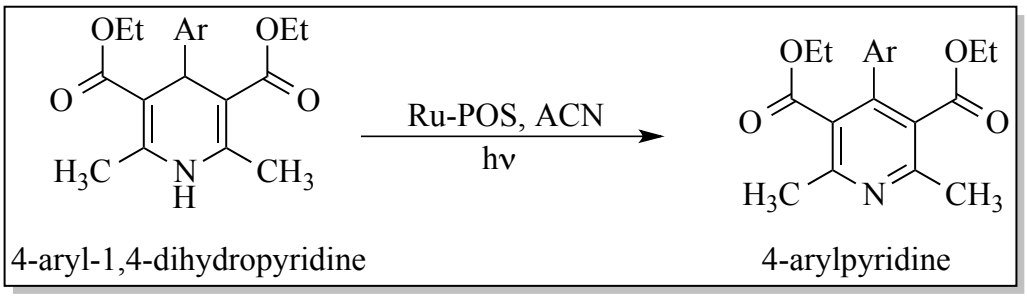

Scheme S3. Photo-catalytic oxidative aromatization of 4-aryldihydropyridine to 4-arylpyridine.

Diethyl 2,6-dimethyl-4-phenylpyridine-3,5-dicarboxylate: ^{1}H NMR ($CDCl_3$, 300 MHz) δ = 7.31-7.11 (m, 5H), 4.16-4.06 (m, 4H), 2.35 (s, 6H), 1.26-1.22 (t, J = 6.9 Hz, 6H); ^{13}C NMR ($CDCl_3$, 75 MHz) δ = 167.6, 147.7, 143.8, 128.0, 127.8, 126.1, 104.2, 59.7, 39.6, 19.6, 14.2.

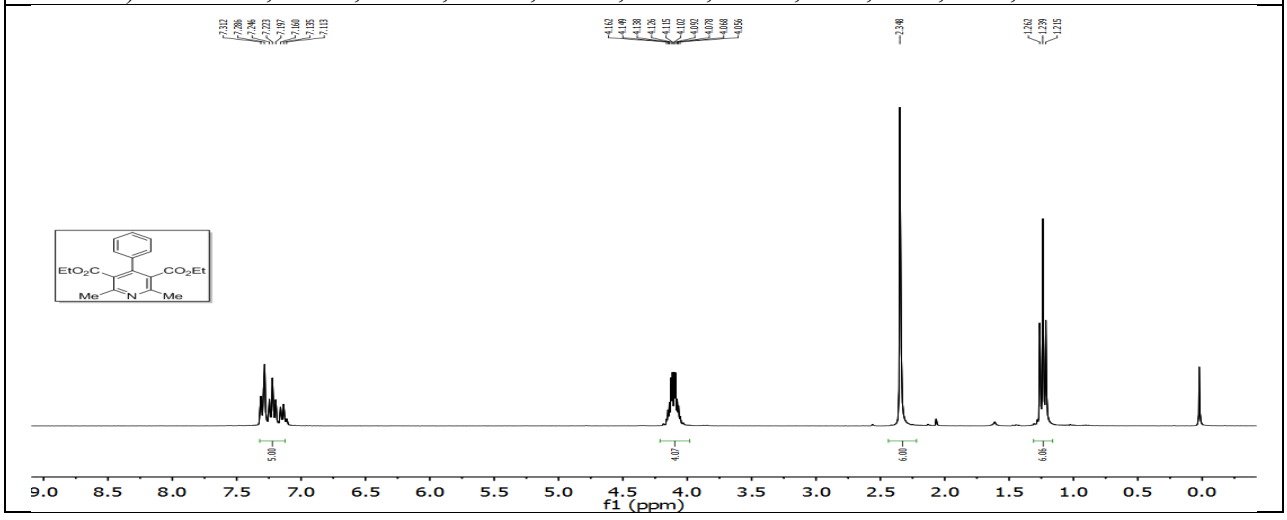

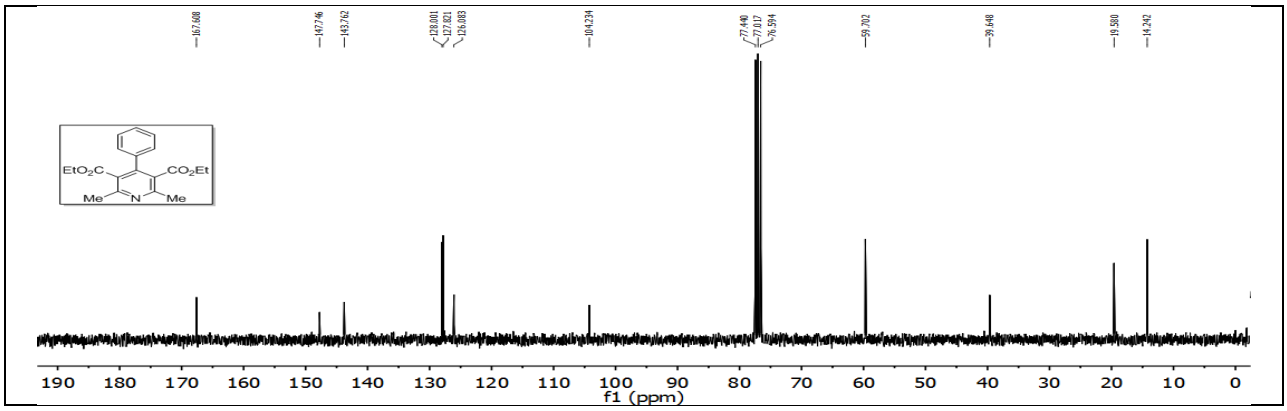
167.688
147.746
143.762
128.001
127.821
126.883
104.234
77.440
77.017
76.594
59.702
39.648
19.580
14.242
EtO2C
CO2Et
Me
N
Me
190 180 170 160 150 140 130 120 110 100 90 80 70 60 50 40 30 20 10 0
f1 (ppm)

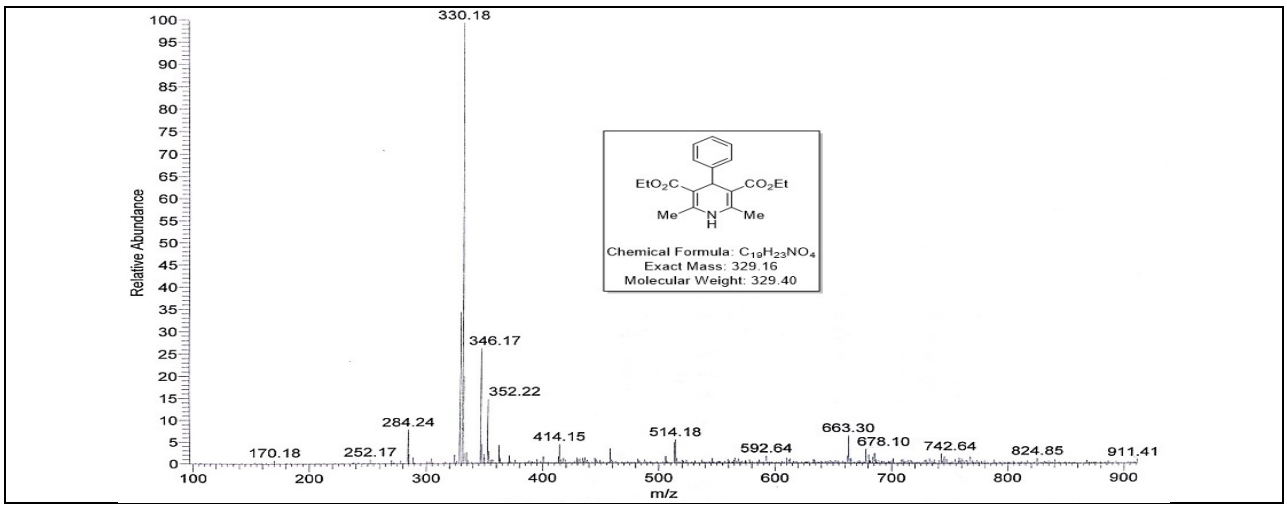
330.18
346.17
352.22
284.24
170.18
252.17
414.15
514.18
592.64
663.30
678.10
742.64
824.85
911.41
Relative Abundance
m/z
EtO2C
CO2Et
Me
N
H
Me
Chemical Formula: C19H23NO4
Exact Mass: 329.16
Molecular Weight: 329.40

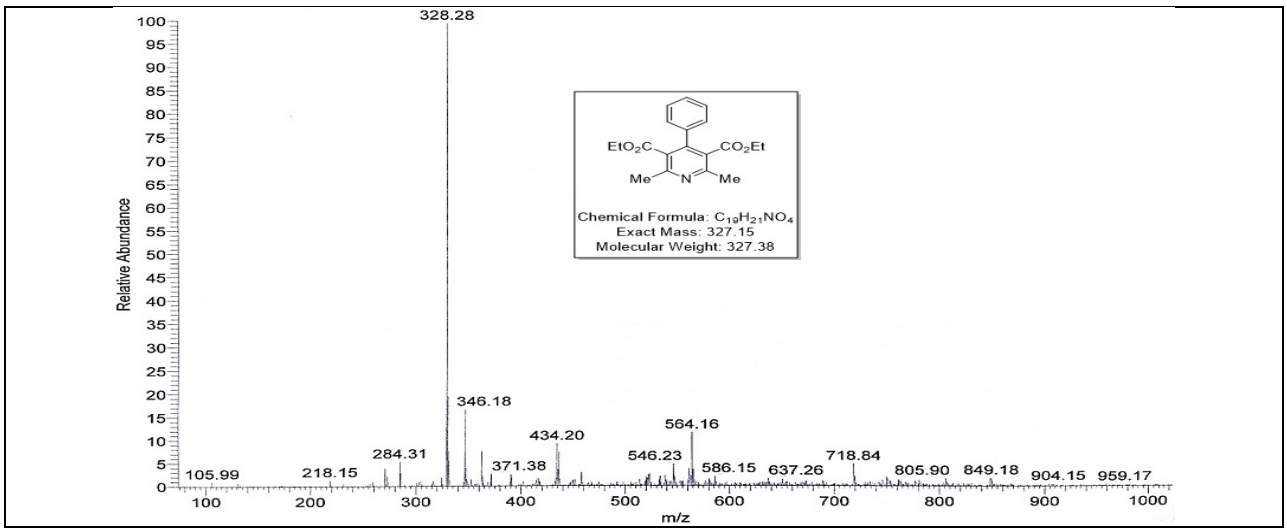
328.28
346.18
564.16
434.20
284.31
371.38
546.23
586.15
637.26
718.84
805.90
849.18
904.15
959.17
105.99
218.15
Relative Abundance
m/z
EtO2C
CO2Et
Me
N
Me
Chemical Formula: C19H21NO4
Exact Mass: 327.15
Molecular Weight: 327.38

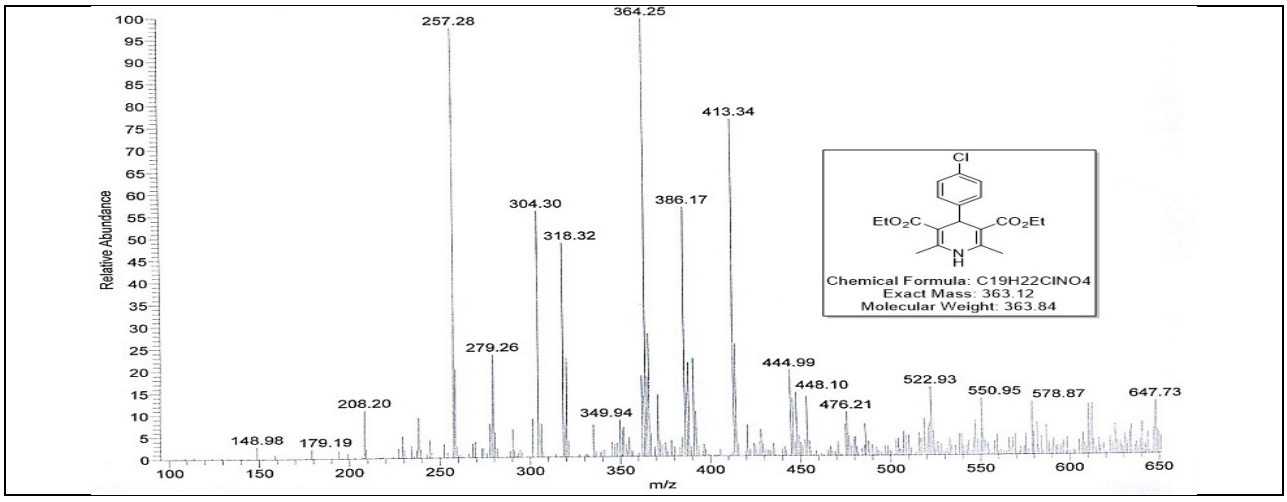
Relative Abundance
m/z
257.28
364.25
413.34
304.30
386.17
318.32
279.26
444.99
448.10
522.93
550.95
578.87
647.73
476.21
208.20
349.94
148.98
179.19
Chemical Formula: C19H22ClNO4
Exact Mass: 363.12
Molecular Weight: 363.84

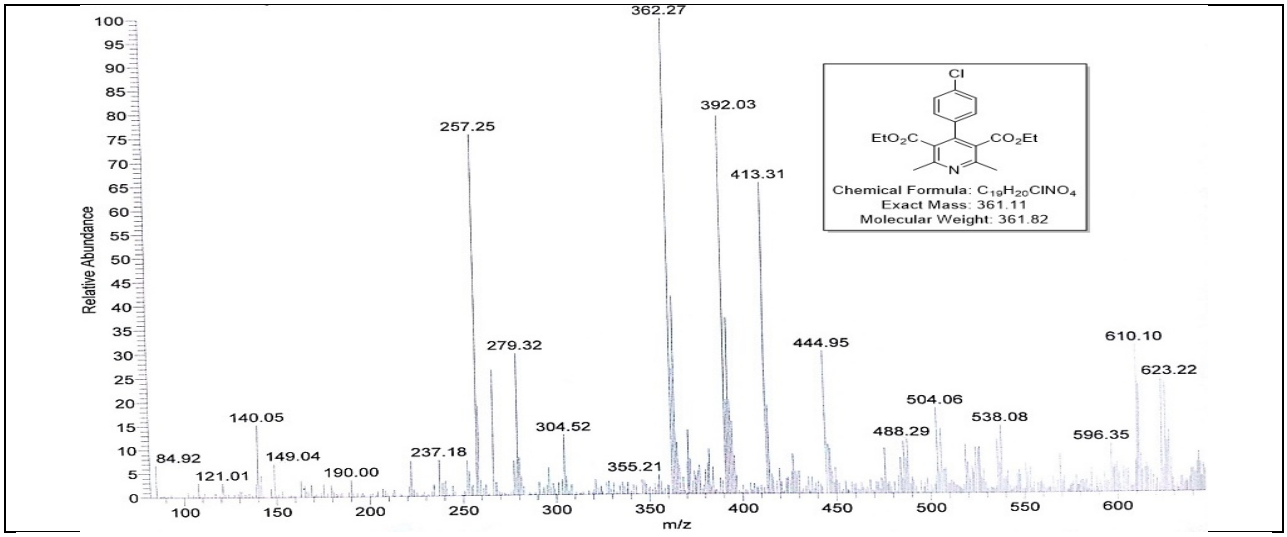
Relative Abundance
m/z
362.27
392.03
257.25
413.31
279.32
444.95
610.10
623.22
504.06
538.08
140.05
304.52
488.29
596.35
84.92
149.04
237.18
121.01
190.00
355.21
Chemical Formula: C19H20ClNO4
Exact Mass: 361.11
Molecular Weight: 361.82

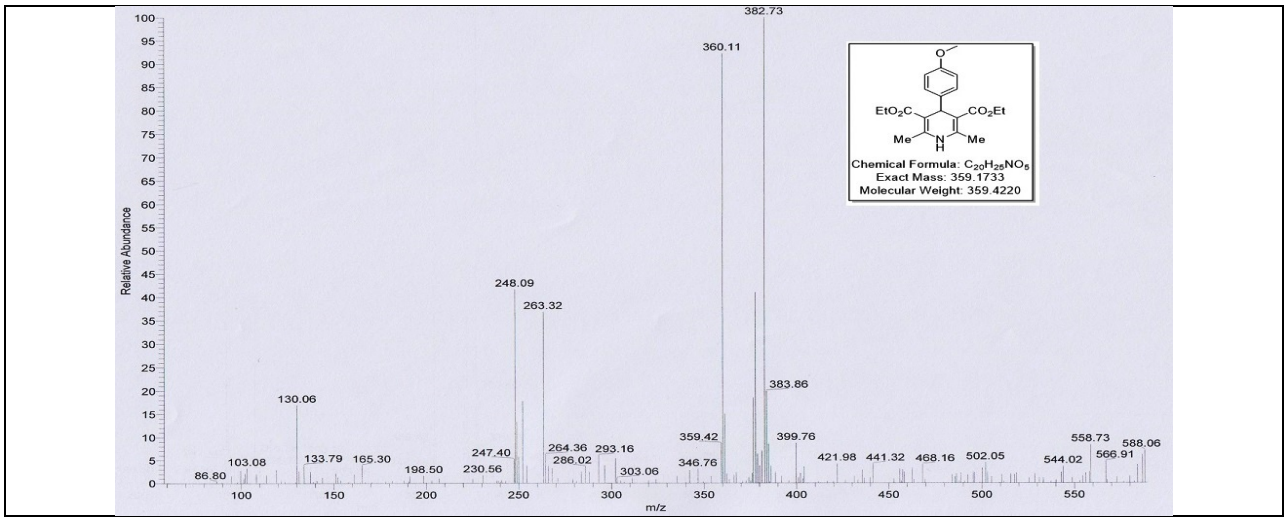
Relative Abundance
m/z
382.73
360.11
248.09
263.32
383.86
130.06
359.42
399.76
558.73
588.06
247.40
264.36
293.16
286.02
346.76
421.98
441.32
468.16
502.05
544.02
566.91
103.08
133.79
165.30
198.50
230.56
303.06
86.80
Chemical Formula: C20H25NO5
Exact Mass: 359.1733
Molecular Weight: 359.4220

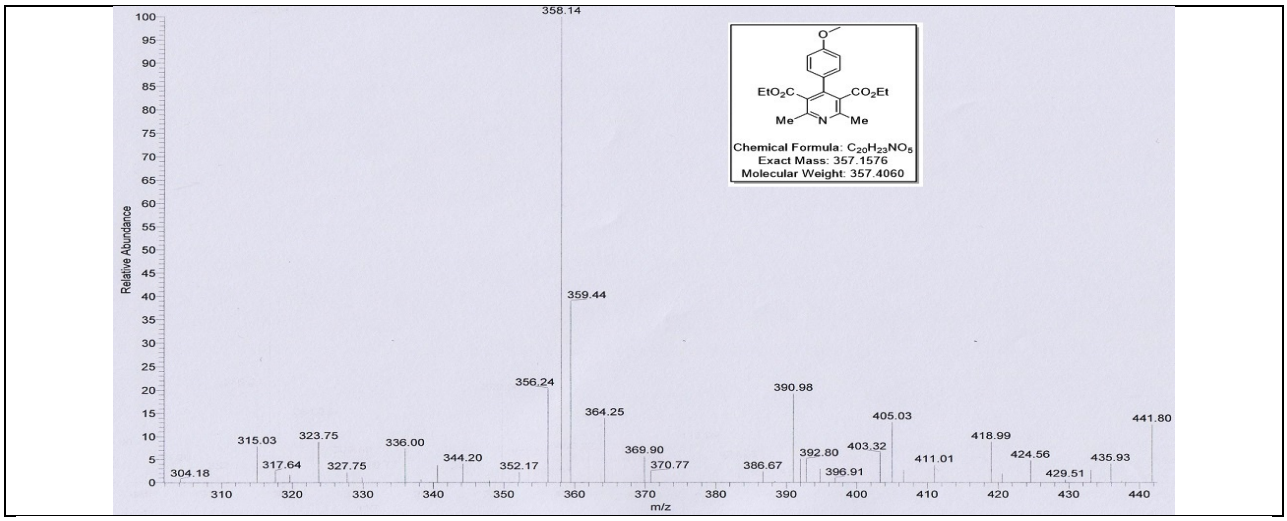
Relative Abundance
m/z
Chemical Formula: C20H23NO5
Exact Mass: 357.1576
Molecular Weight: 357.4060

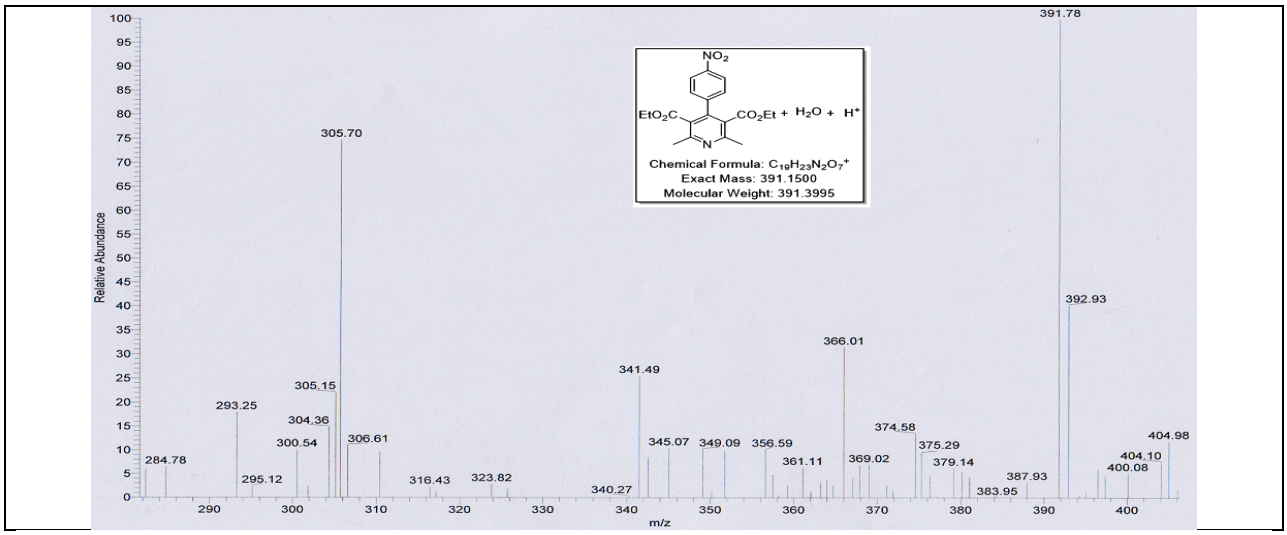
Relative Abundance
m/z
Chemical Formula: C19H23N2O7+
Exact Mass: 391.1500
Molecular Weight: 391.3995

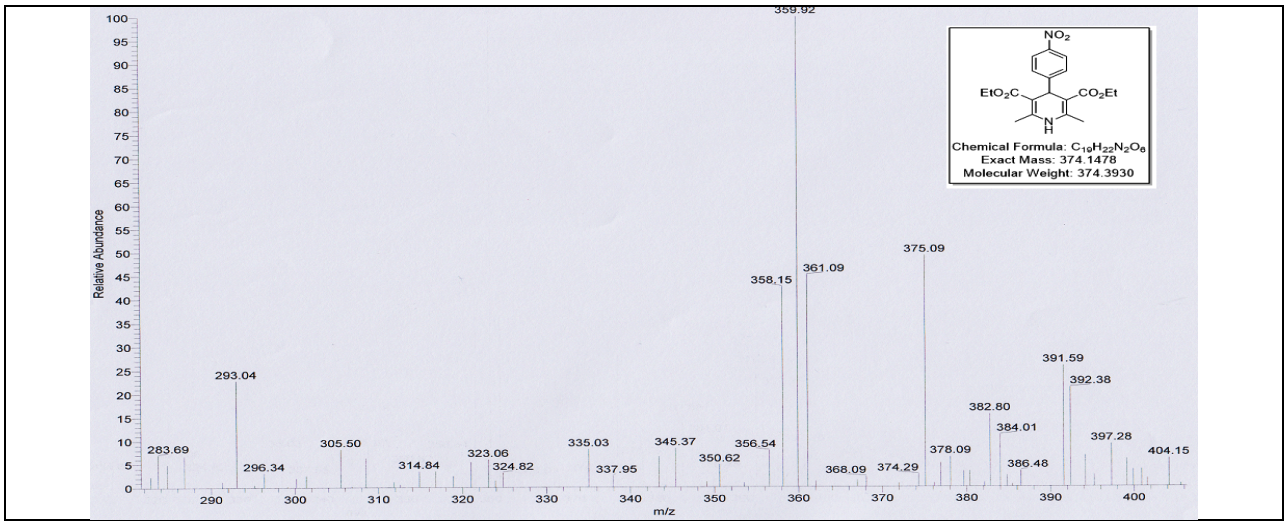
Relative Abundance
m/z
Chemical Formula: C19H22N2O6
Exact Mass: 374.1478
Molecular Weight: 374.3930

Synthesis of 1,2-dihydropyridine derivatives: The corresponding 1,2-dihydropyridine derivatives were synthesized by following the literature procedure as shown in Scheme S4.[5]

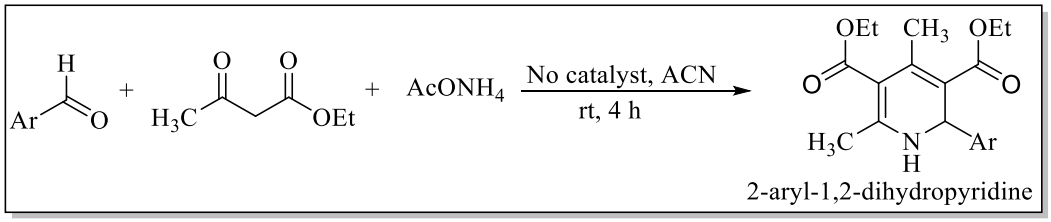

Scheme S4. Synthesis of 1,2-dihydropyridine derivatives.

Photo-catalytic oxidative aromatization of 1,2-dihydropyridine derivatives: The photo-catalytic oxidative aromatization of 1,2-dihydropyridine derivatives was carried out by following the same procedure as described under the section "*Photo-catalytic oxidative aromatization of 1,4-dihydropyridine derivatives"*.

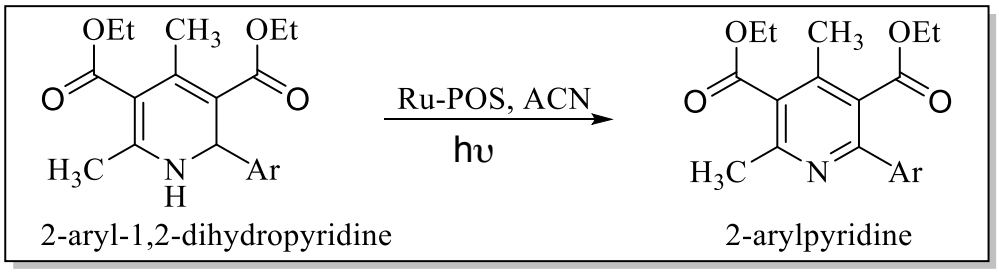

Scheme S5. Photo-catalytic oxidative aromatization of 1,2-dihydropyridine derivatives to 2-arylpyridines.

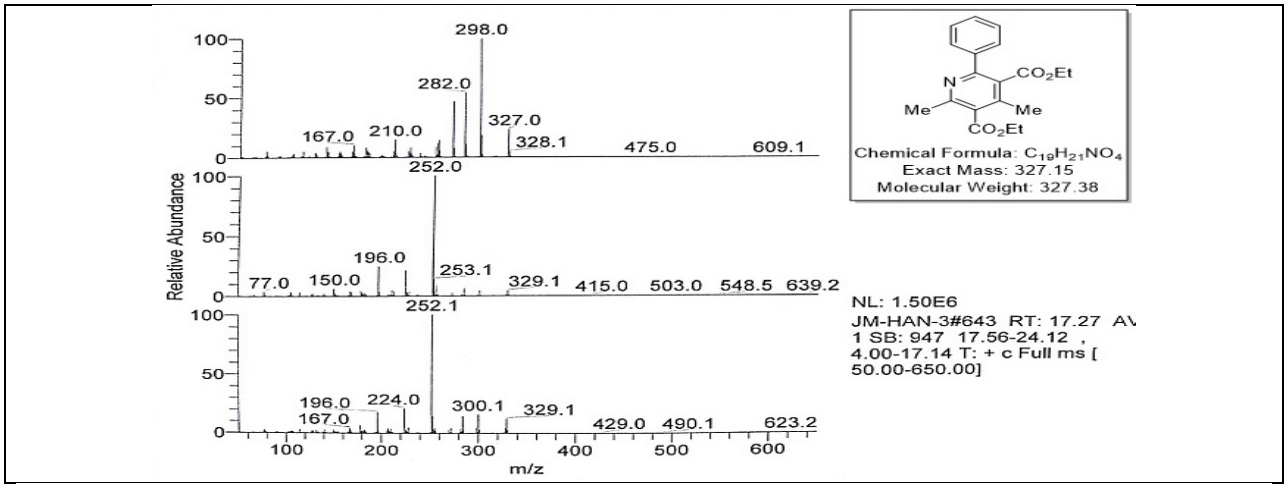

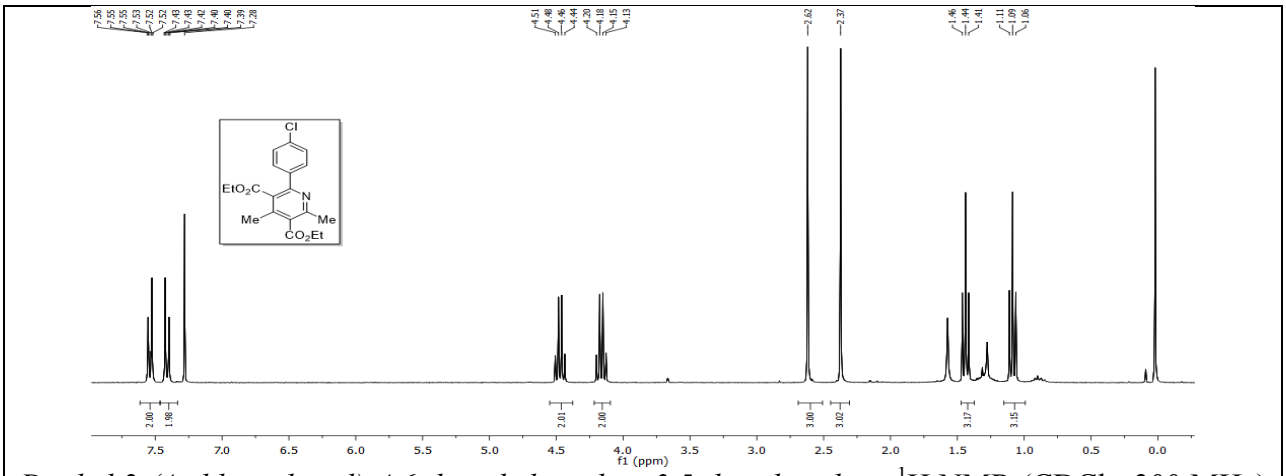

Diethyl 2-(4-chlorophenyl)-4,6-dimethylpyridine-3,5-dicarboxylate: ^{1}H NMR ($CDCl_3$, 300 MHz) δ = 7.55-7.52 (m, 2H), 7.43-7.39 (m, 2H), 4.51-4.44 (q, J = 7.2 Hz, 2H), 4.19 (4.13 (q, J = 7.2 Hz, 2H), 2.62 (s, 3H), 2.37 (s, 3H), 1.46-1.42 (t, J = 6.9 Hz, 3H), 1.11-1.06 (t, J = 6.9 Hz, 3H).

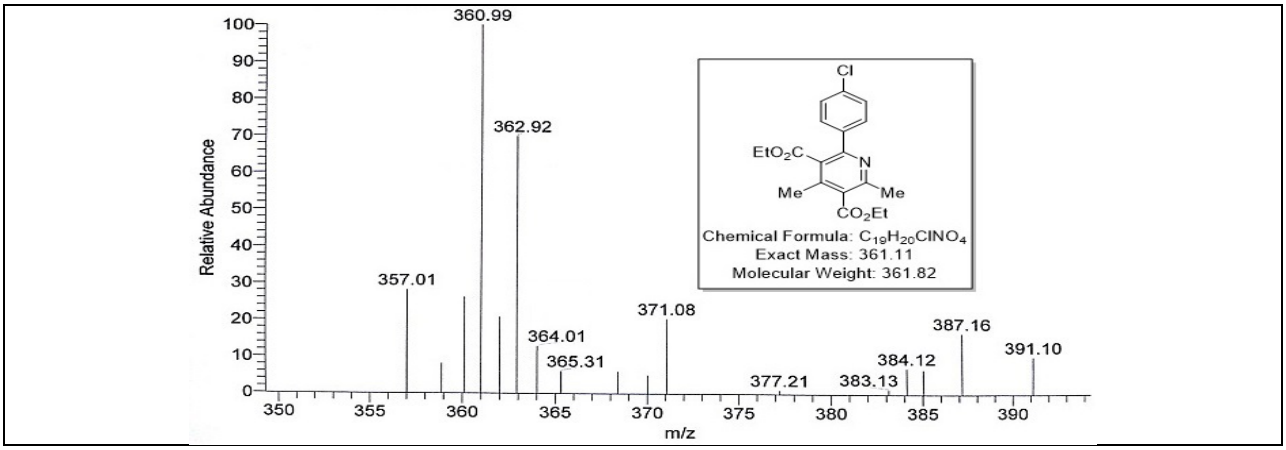

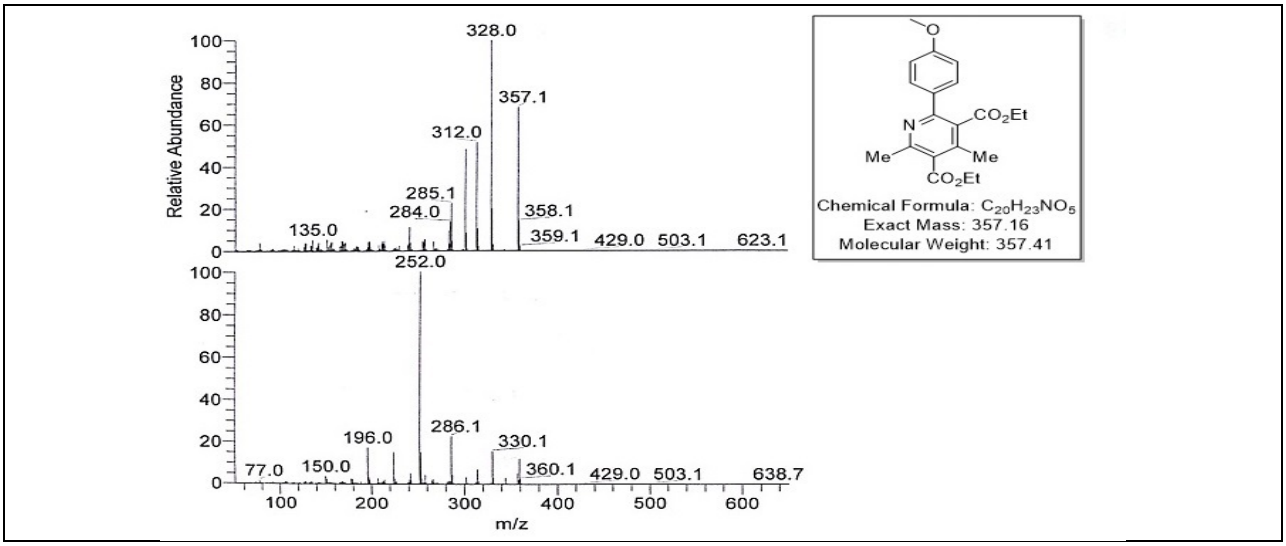

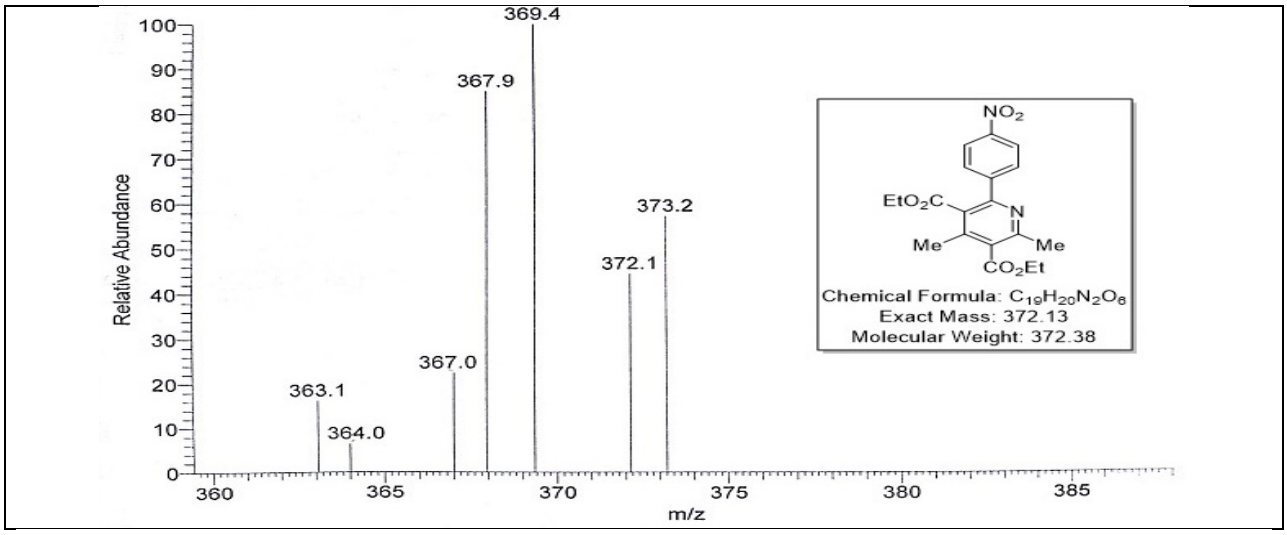

Reductive dehalogenation of alkyl halide to alkane: Alkyl halide (1 mmol), dihydropyridine i.e., diethyl 2,6-dimethyl-4-phenyl-1,4-dihydropyridine-3,5-dicarboxylate (1.1 mmol), and $^{i}Pr_2NEt$ (2 mmol) were dissolved in dry DMF (10 mL), and then Ru-POS (20 mg) was added in the suspension. The reaction was irradiated using 25W compact fluorescent lamp for 3 h.

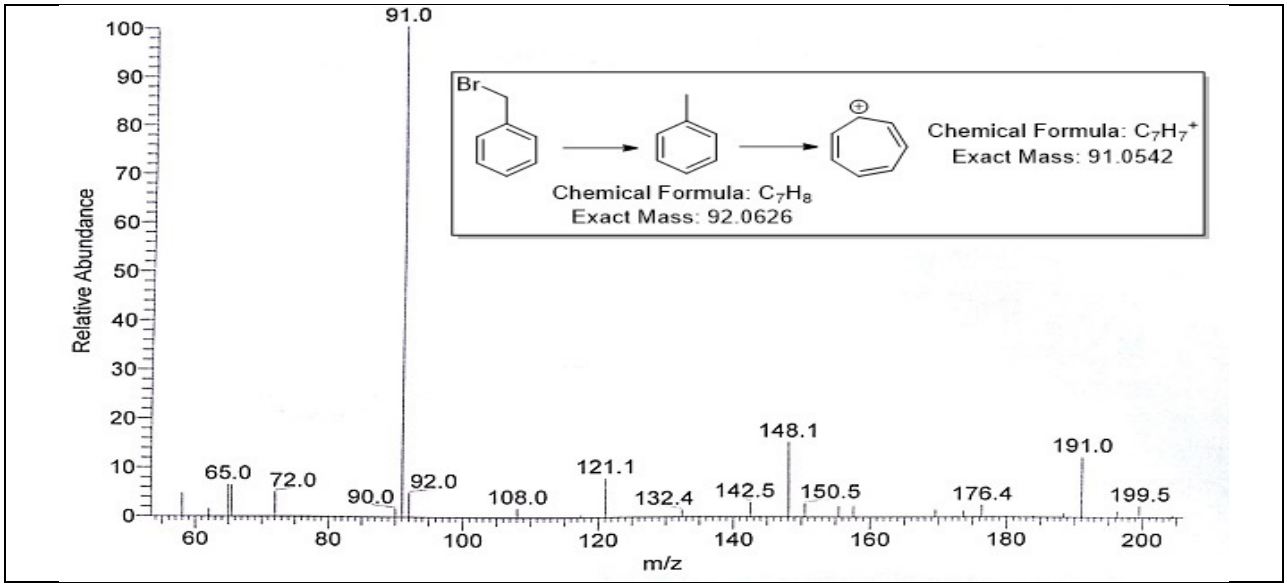

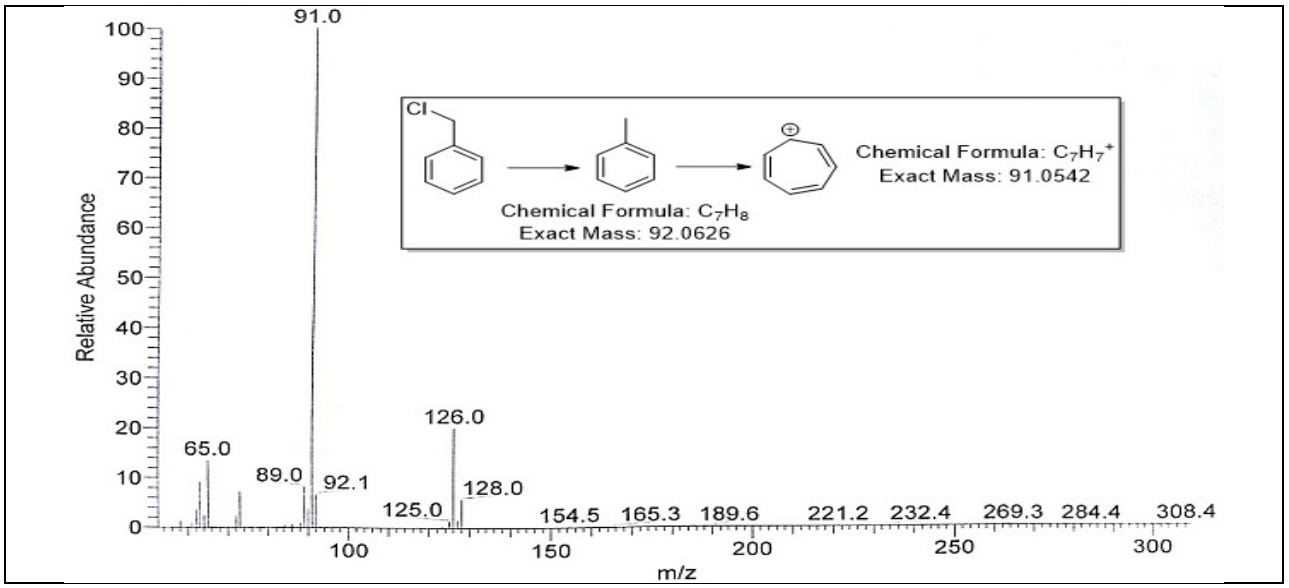
91.0
Relative Abundance
m/z
65.0
89.0
92.1
125.0
126.0
128.0
154.5
165.3
189.6
221.2
232.4
269.3
284.4
308.4
Cl
Chemical Formula: C_7H_8
Exact Mass: 92.0626
Chemical Formula: $C_7H_7^+$
Exact Mass: 91.0542

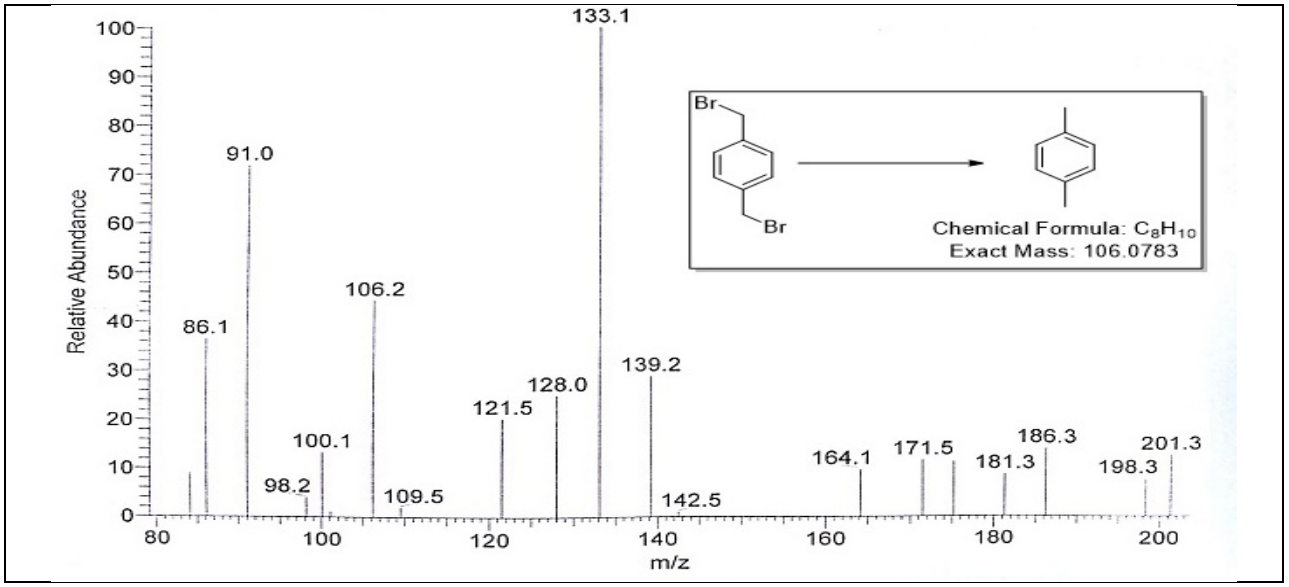
133.1
91.0
Relative Abundance
m/z
86.1
106.2
98.2
100.1
109.5
121.5
128.0
139.2
142.5
164.1
171.5
181.3
186.3
198.3
201.3
Br
Br
Chemical Formula: C_8H_{10}
Exact Mass: 106.0783

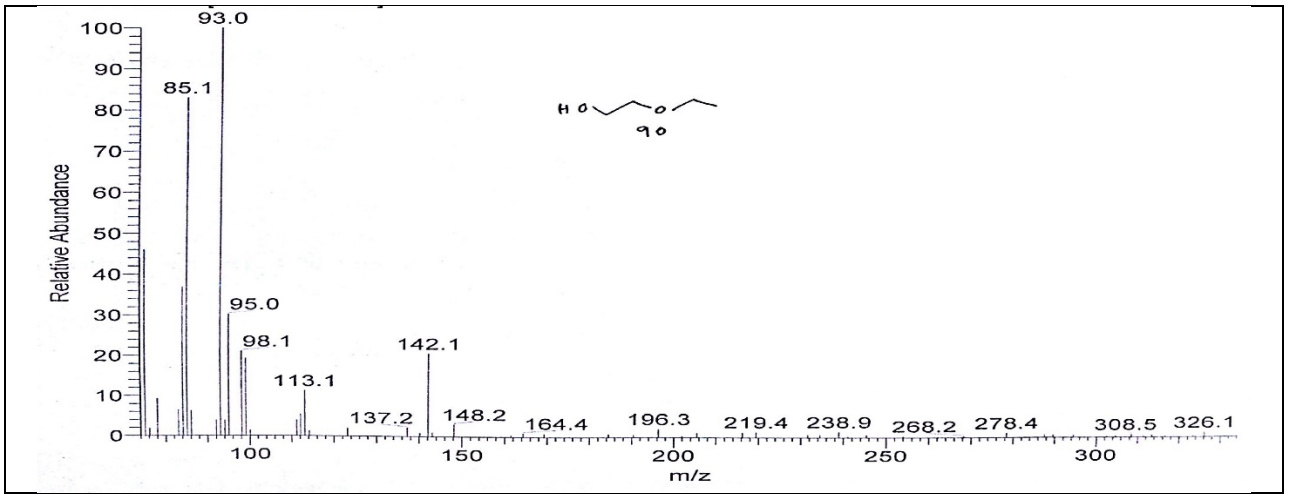
93.0
85.1
Relative Abundance
m/z
95.0
98.1
113.1
137.2
142.1
148.2
164.4
196.3
219.4
238.9
268.2
278.4
308.5
326.1

Functional group interconversion (FGI) of alcohol to alkyl halide:

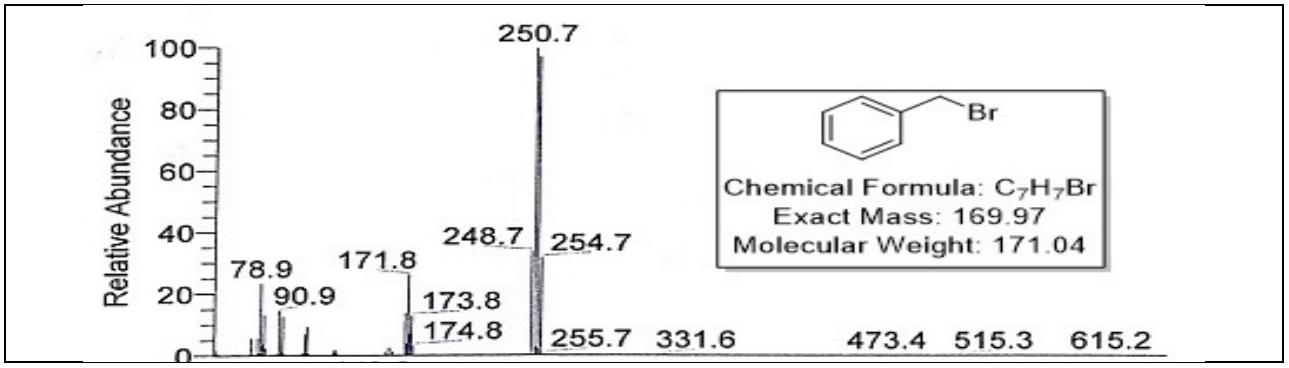

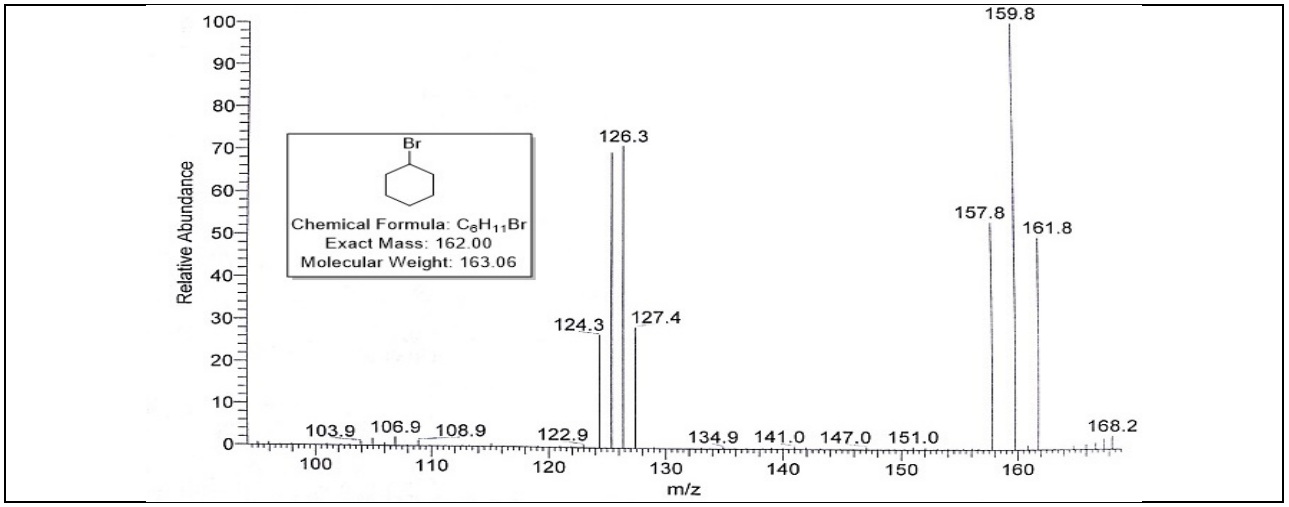

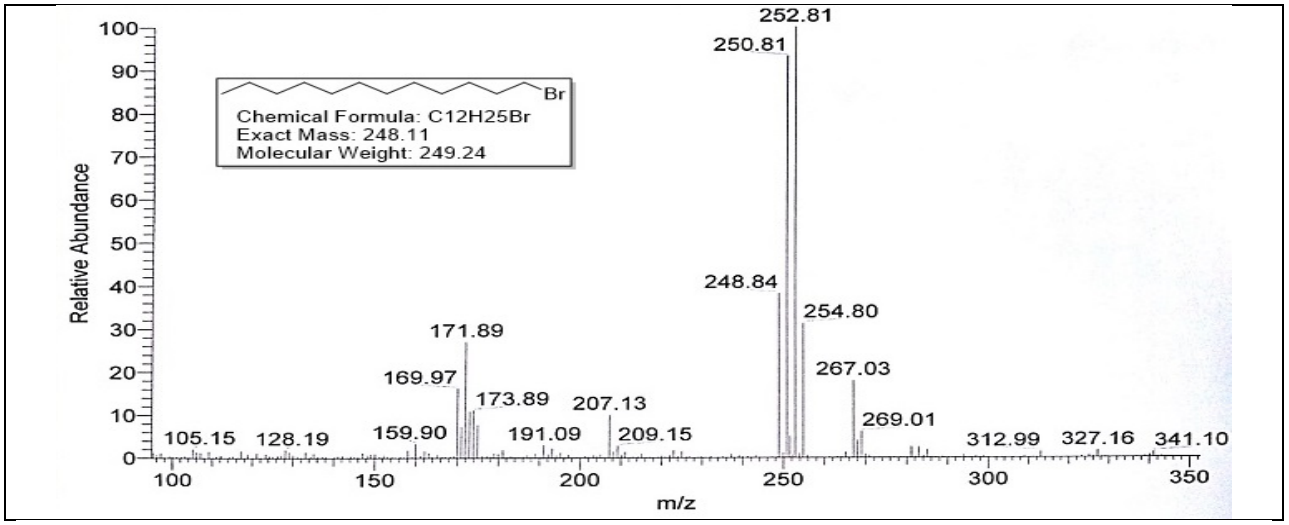

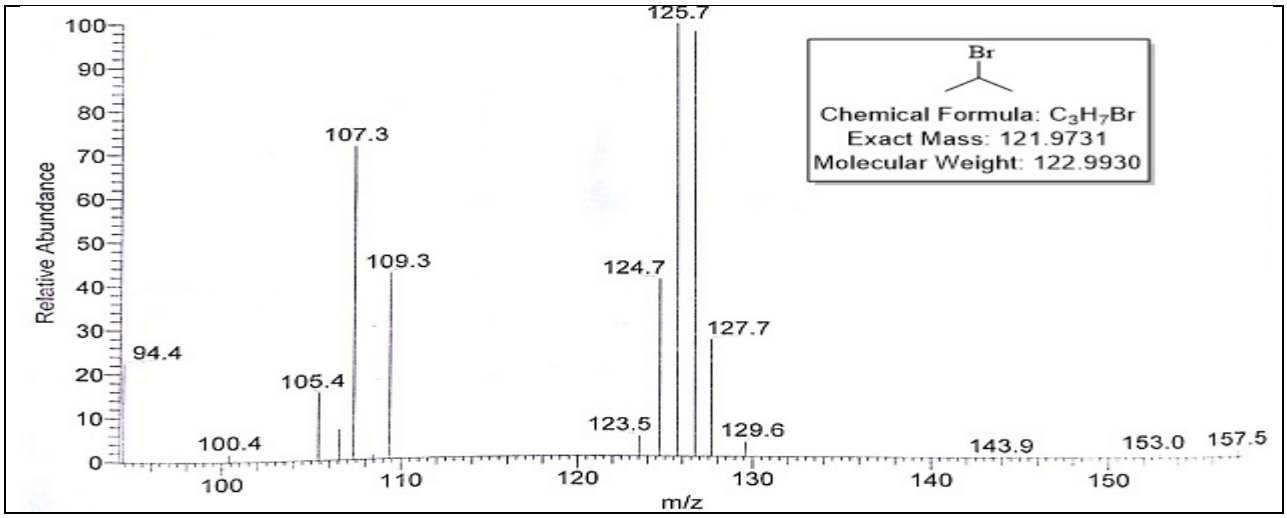
Br
Chemical Formula: C_3H_7Br
Exact Mass: 121.9731
Molecular Weight: 122.9930
Relative Abundance
m/z
125.7
107.3
109.3
124.7
127.7
94.4
105.4
123.5
129.6
100.4
143.9
153.0
157.5

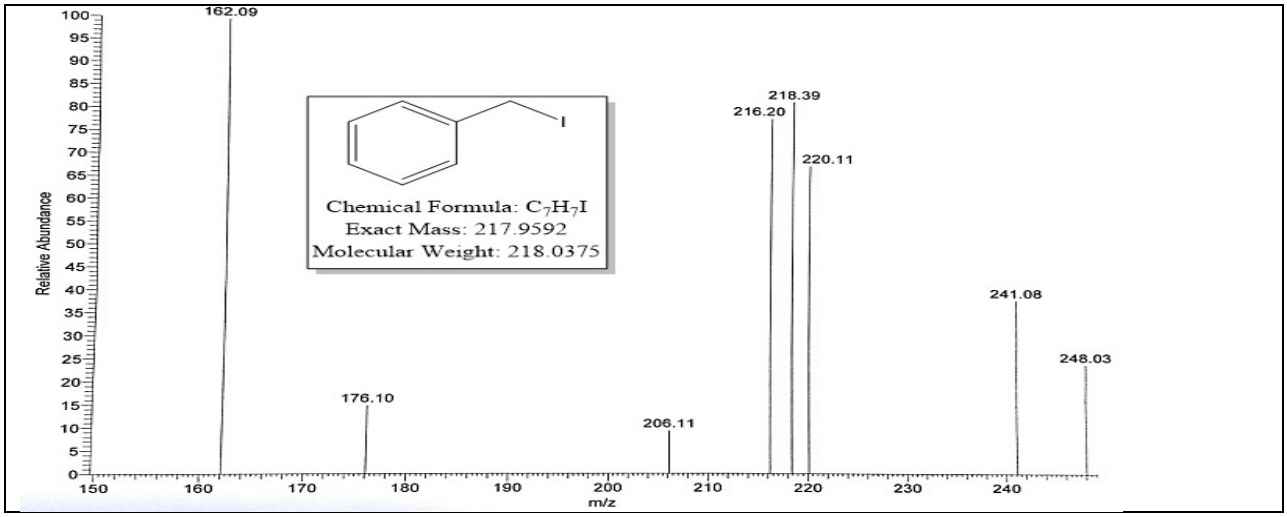
I
Chemical Formula: C_7H_7I
Exact Mass: 217.9592
Molecular Weight: 218.0375
Relative Abundance
m/z
162.09
218.39
216.20
220.11
241.08
248.03
176.10
206.11

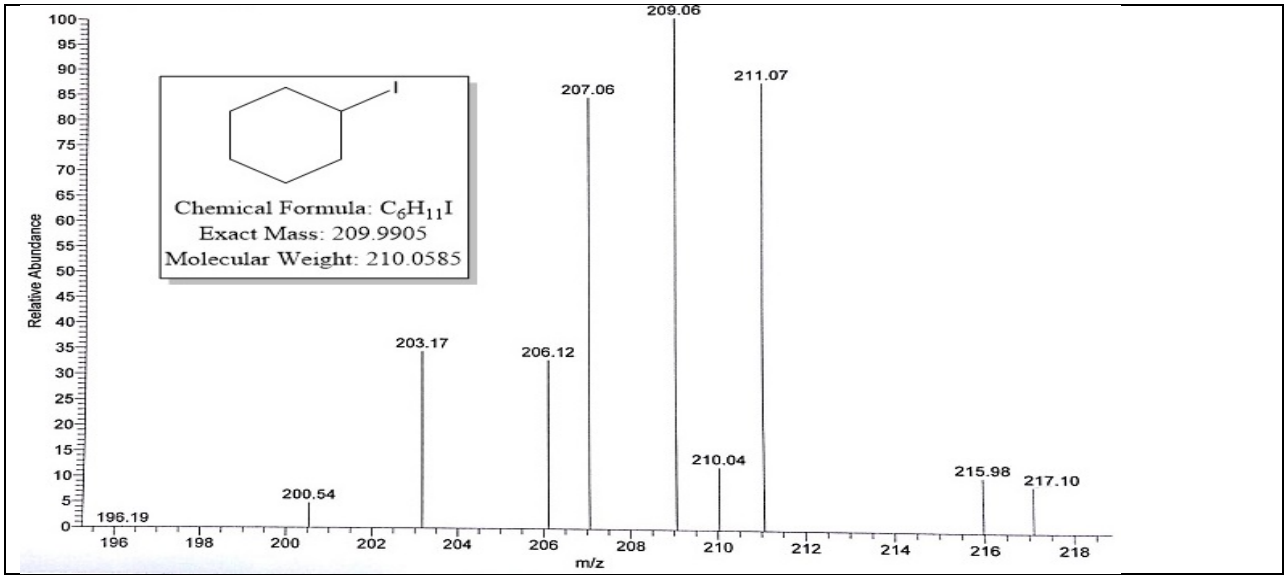
I
Chemical Formula: $C_6H_{11}I$
Exact Mass: 209.9905
Molecular Weight: 210.0585
Relative Abundance
m/z
209.06
207.06
211.07
203.17
206.12
210.04
215.98
217.10
200.54
196.19

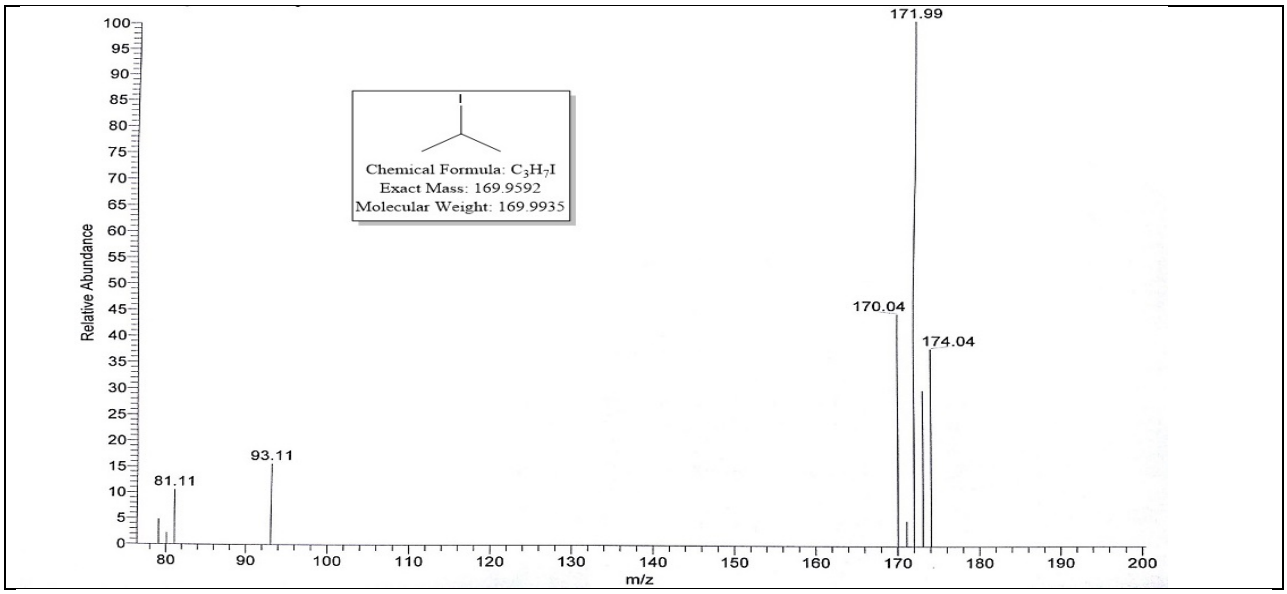
Chemical Formula: C_3H_7I
Exact Mass: 169.9592
Molecular Weight: 169.9935
171.99
170.04
174.04
93.11
81.11
Relative Abundance
m/z

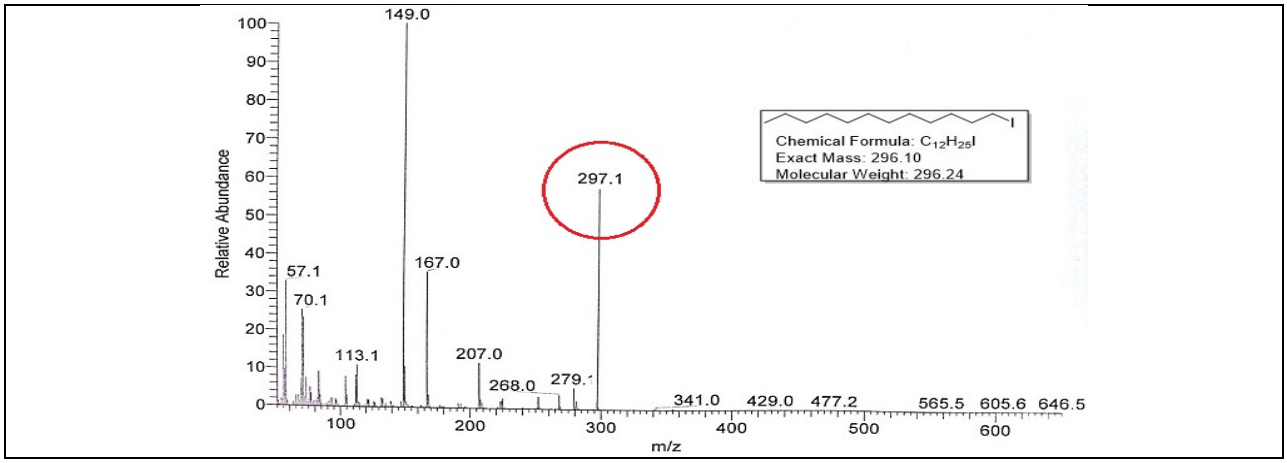
Chemical Formula: $C_{12}H_{25}I$
Exact Mass: 296.10
Molecular Weight: 296.24
149.0
297.1
167.0
57.1
70.1
113.1
207.0
268.0
341.0
429.0
477.2
565.5
605.6
646.5
Relative Abundance
m/z

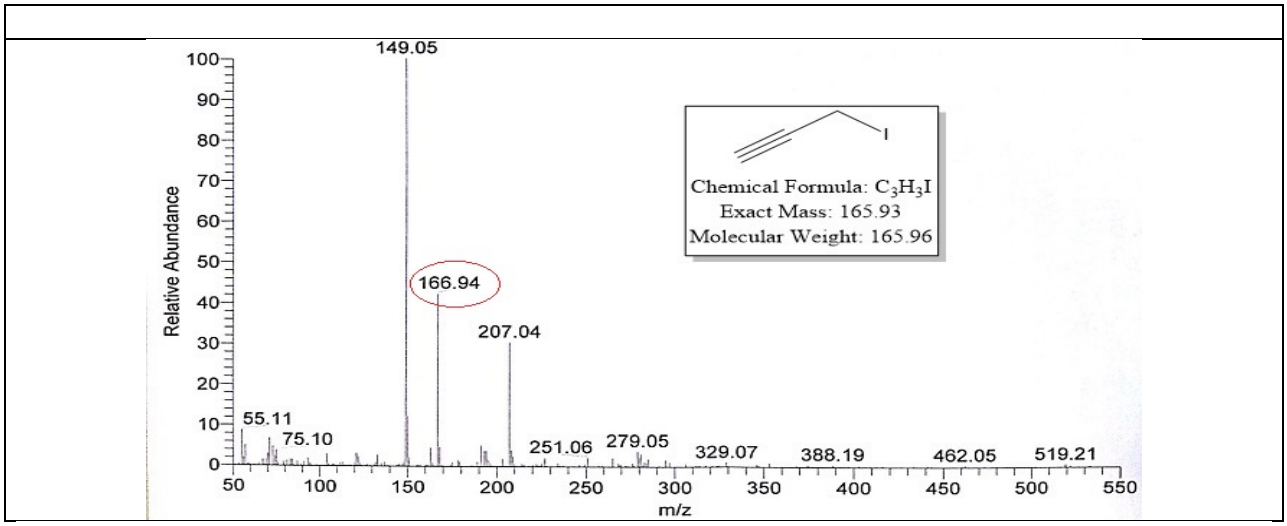
Chemical Formula: C_3H_3I
Exact Mass: 165.93
Molecular Weight: 165.96
149.05
166.94
207.04
55.11
75.10
251.06
279.05
329.07
388.19
462.05
519.21
Relative Abundance
m/z

Reusability and durability test for Ru-POS:

By employing the optimized reaction conditions, the oxidative aromatization of Hantzsch ester to yield the pyridine derivative **4a** was carried out again to demonstrate the durability and recyclability of Ru-POS during 10 successive catalytic cycles. For this study, Ru-POS (20 mg) was used for the catalyst recycling experiment. The recovery rate of the catalyst after each catalytic cycle was calculated after drying it at 60 °C. The catalyst was recycled and reused for ten repetitive catalytic cycles without a significant loss of catalytic activity, and the catalyst was recovered in a constant rate in each catalytic cycle (Figure S9).

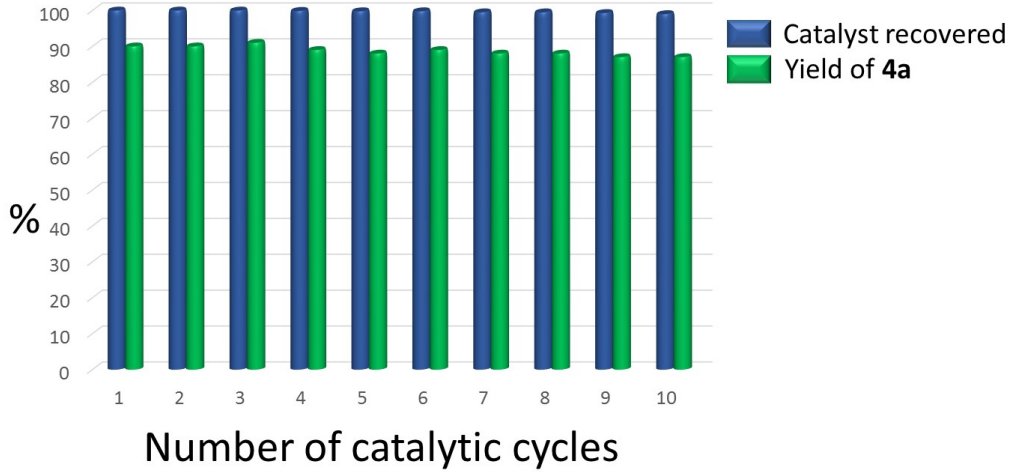

Figure S9. Recycling potential of Ru-POS.

Leaching test: In order to investigate heterogeneous nature of the catalyst, leaching test was performed using the oxidative aromatization of Hantzsch ester to yield the pyridine derivative **4a**. After 1 h of the reaction, reaction was stopped and the catalyst was separated by simple filtration technique. After 1 h, 60% product conversion was achieved (confirmed by GC-MS analysis). Then, we carried out the catalytic reaction to treat the filtrate with light irradiation. But no increase in the product conversion beyond 60% was achieved. This experimental result signifies that the catalyst is truly heterogeneous in nature and ruthenium bipyridyl complex was strongly anchored inside the pore wall of Ru-POS. That is why no leaching of Ru took place in the reaction mixture during the course of the catalytic reaction. We checked the filtrate employing AAS (Atomic Absorption Technique) but no trace amount of Ru was present there. We also checked Ru content in Ru-POS after 10^{th} catalytic cycle employing ICP-MS technique. Ru content in reused Ru-POS material is 0.048 mmol/g.

Characterization of reused Ru-POS catalyst after 10th catalytic cycle:

We characterized the reused Ru-POS catalyst after 10th catalytic cycle employing ^{13}C CP MAS NMR (Figure S2), FT-IR (Figure S3), XPS (Figure S5d) and HR-TEM (Figure S7d) tools. ^{13}C CP MAS NMR and FT-IR spectra of the used catalyst were found to be similar to that of the as-synthesized Ru-POS, proving the integrity of the $Ru(bpy)_3$ complex structure throughout the catalytic reaction. HR-TEM analysis reveals that the mesophase of the catalyst was unaffected and the XPS analysis shows that the +2 oxidation of the $Ru(bpy)_3$ complex was preserved even after 10 catalytic cycles.

Effect of catalyst dose on oxidative aromatization of Hantzsch ester to yield compound 4a

The effect of the catalyst dose for the synthesis of compound **4a** is depicted in Figure S10. It was evident that 20 mg of the catalyst was the effective amount required to carry out the reaction. No substantial change in the product yield was observed with the increase of the catalyst dose.

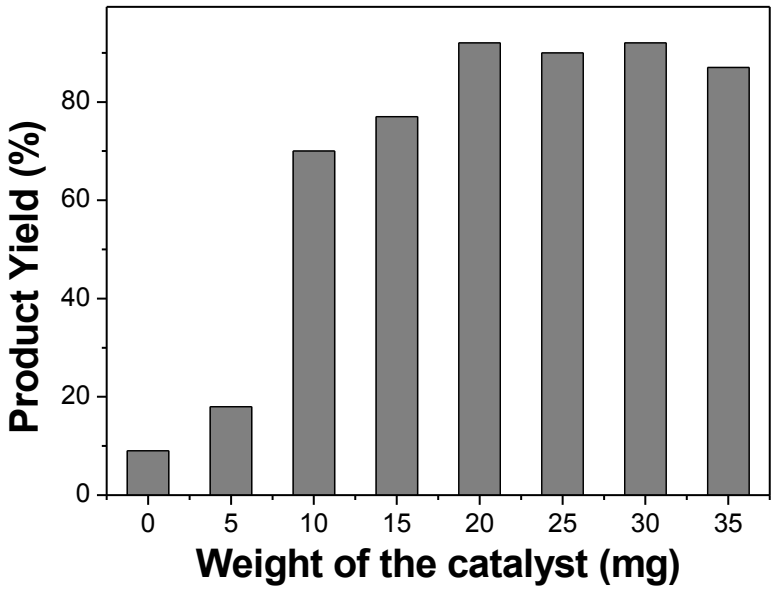

Figure S10. Effect of the catalyst dose on the product yield of compound **4a**.

References:

1. J. Ohkanda, R. Satoh and N. Kato, *Chem. Commun*., 2009, **45**, 6949–6951.
2. I. G. Gauthier, F. Odobel, M. Alebbi, R. Argazzi, E. Costa, C. A. Bignozzi, P. Qu and G. J. Meyer, *Inorg. Chem.,* 2001, **40***,* 6073-6079.
3. J. Mondal, A. Modak, M. Nandi, H. Uyama and A. Bhaumik, *RSC Adv.,* 2012, **2**, 11306–11317.
4. A. Debache, W. Ghalem, R. Boulcina, A. Belfaitah, S. Rhouati and B. Carboni, *Tetrahedron Lett*., 2009, **50**, 5248–5250.
5. R. Ananthakrishnan and S. Gazi, *Catal. Sci. Technol.,* 2012, **2**, 1463–1471.